BENCHMARK COMPARISON REPORT

Computational Fluid x-Dynamics (CFxD)
(Version 2.08.09, June 9, 2026)

2026

Contents

Nomenclature

Symbol	Dimension	Definition
C_i , c_i		model coefficients
c_p	$J/(kg\times K)$	specific heat capacity by constant pressure
g_i	m/s^2	gravity acceleration
Kn		Knudsen number
k	m^2/s^2	turbulent kinetic energy
l	m	characteristic length scale
M		Mach number
m	kg	mass
Nu		Nusselt number
P_k		turbulent production
Pr		Prandtl number
Pr_t		Prandtl turbulent number
p	Pa	static pressure
R	$J/(kg\times K)$	gas constant
Re		Reynolds number
Sc		Schmidt number
T	K	temperature
t	s	time
u, u_i	m/s	velocity vector/components
$\overline{u_i'u_j'}$	m^2/s^2	Reynolds stress tensor (components)
$\overline{u_j'\varphi'}$		scalar flux (components)
V	m^3	volume
x_i	m	cartesian coordinates

Greek letters

Symbol	Dimension	Definition
$\alpha_i, \beta_i, \delta_i, \gamma_i$		model coefficients
$\dot{\gamma}$		strain rate

Γ_φ		Molecular diffusion coefficient of a general scalar quantity, φ
δ_{ij}		Cartesian components of unit tensor (Kronecker delta)
ε	m^2/s^2	dissipation rate of turbulent kinetic energy
λ	$J/(s\times K\times m)$	thermal conductivity
φ		general scalar quantity
κ		Karman constant
μ, μ_t	$kg/(m\times s)$	dynamic molecular/turbulent viscosity
ν, ν_t	m^2/s	kinematic molecular/ turbulent viscosity
ρ	kg/m^3	density
σ	m^2	surface
σ_φ		turbulent Schmidt (or Prandtl) number for variable
τ	s	turbulent time scale
τ_{ij}		Reynolds stress tensor (components)
ω		specific dissipation rate

Abbreviations

Abbreviation	Definition
CAD	Computer-aided design
CDS	Central Difference Scheme
CFD	Computational Fluid Dynamics
CV	Control Volume
DNS	Direct Numerical Simulation
EVM	Eddy-Viscosity Model
LES	Large Eddy Simulation
RANS	Reynolds Averaged Navier-Stokes
RSM	Reynolds Stress Model
SIMPLE	Semi Implicit Method for Pressure Linked Equations
UDS	Upwind Difference Scheme
URANS	Unsteady RANS

Introduction

Computational Fluid Dynamics (CFD) software is widely used to predict fluid flow, heat transfer, and related engineering phenomena. The reliability of a CFD workflow depends not only on the numerical solver, but also on the complete simulation process, including geometry preparation, mesh generation, boundary condition definition, solver setup, convergence monitoring, and post-processing. For this reason, verification and benchmark comparisons are important steps in evaluating the practical performance of a CFD platform.

CFxD is a CFD application developed to provide an integrated workflow for engineering simulations, from geometry creation and meshing to solver execution and result visualization. The software is designed to simplify the setup of CFD cases while maintaining access to established numerical methods and solver technologies. To assess the behavior of CFxD a set of benchmark cases was prepared and compared with results obtained using Ansys Fluent.

The objective of this document is to present a preliminary verification and benchmark comparison between CFxD and Ansys Fluent. The comparison focuses on practical engineering outputs such as velocity fields, temperature distributions, flow profiles, and general solution behavior. Several cases with different mesh types, mesh sizes, and turbulence-model settings are considered. The purpose is not to claim universal equivalence between the two software packages, but to evaluate whether CFxD produces consistent and reasonable results for selected representative cases.

This document should be considered as a technical benchmark report rather than a complete validation study. A full validation study would require comparison against analytical solutions, experimental measurements, or well-established published benchmark data. Nevertheless, comparison with a mature commercial CFD package provides a useful practical reference for evaluating the consistency of CFxD results and demonstrating the current capabilities of the software.

Chapter I. Basic benchmark cases

This chapter presents introductory benchmark cases covering **steady and transient** simulations for **incompressible** and **subsonic compressible (M < 1)** flows, with and without **heat transfer**.

1. Flow in a pipe (incompressible internal flow)

The configuration represents a pipe with a diameter of 0.6 m (D), a 90° bend, and upstream and downstream straight sections with lengths of 5D and 10D, respectively. The inlet velocity is 2 m/s and the fluid is air. The Reynolds number based on the pipe diameter and inlet velocity is approximately $Re = 8.2 \times 10^4$.

The mesh size used for CFxD is approximately 155 thousand cells, while the mesh size used in Fluent is approximately 144 thousand cells. The SST turbulence model is used for both simulations.

Results and comparison

The velocity magnitude contour at the symmetry plane obtained with Fluent and CFxD is shown in Figure 1.

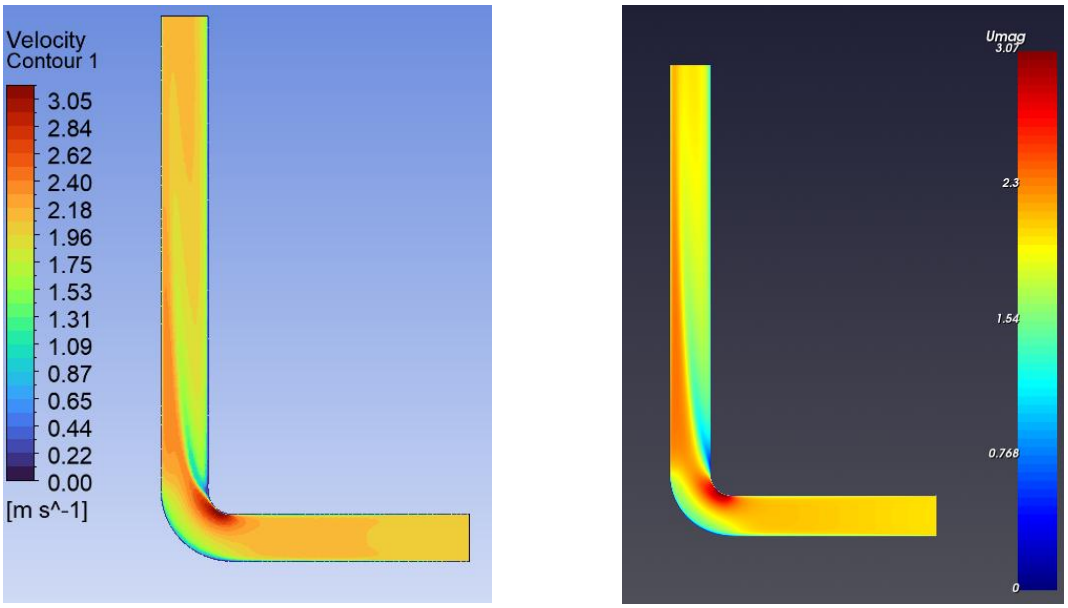

Figure 1. Velocity magnitude contour obtained with Fluent (left) and CFxD (right).

The kinetic energy contour at the symmetry plane obtained with Fluent and CFxD is shown in Figure 2.

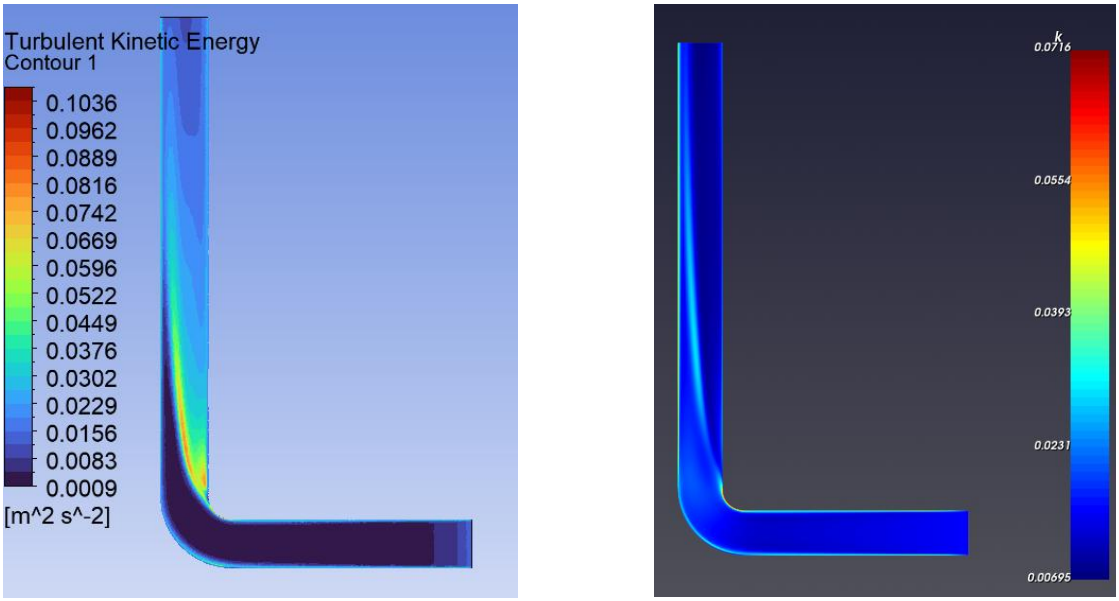

Figure 2. Kinetic energy contour obtained with Fluent (left) and CFxD (right).

The specific dissipation rate contour at the symmetry plane obtained with Fluent and CFxD is shown in Figure 3.

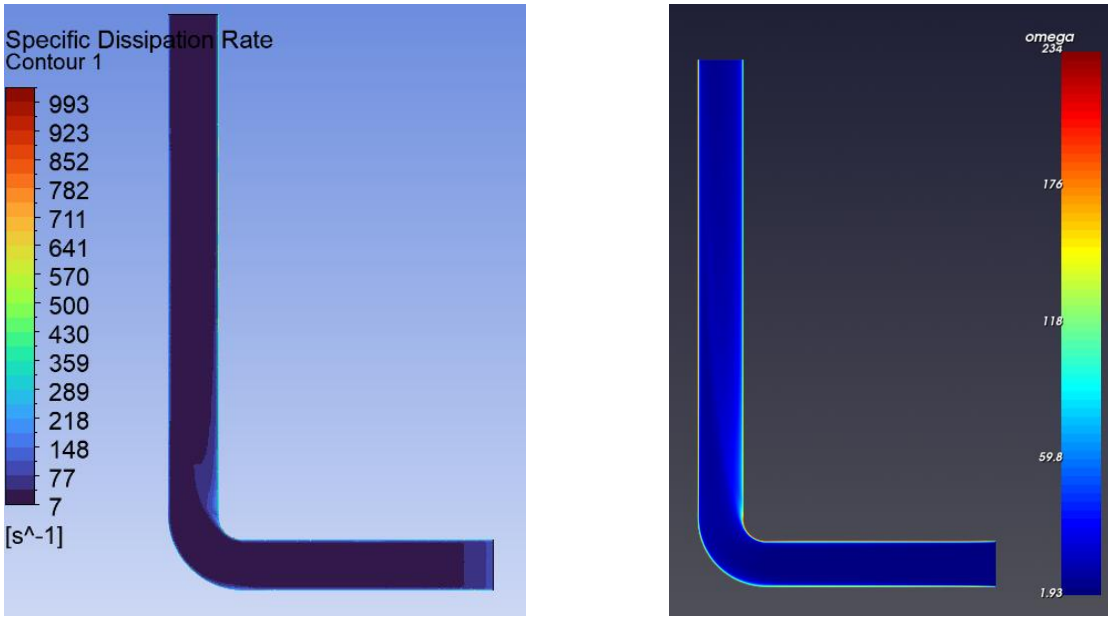

Figure 3. Specific dissipation rate contour obtained with Fluent (left) and CFxD (right).

The velocity vector plots near the pipe bend obtained with Fluent and CFxD are shown in Figure 4.

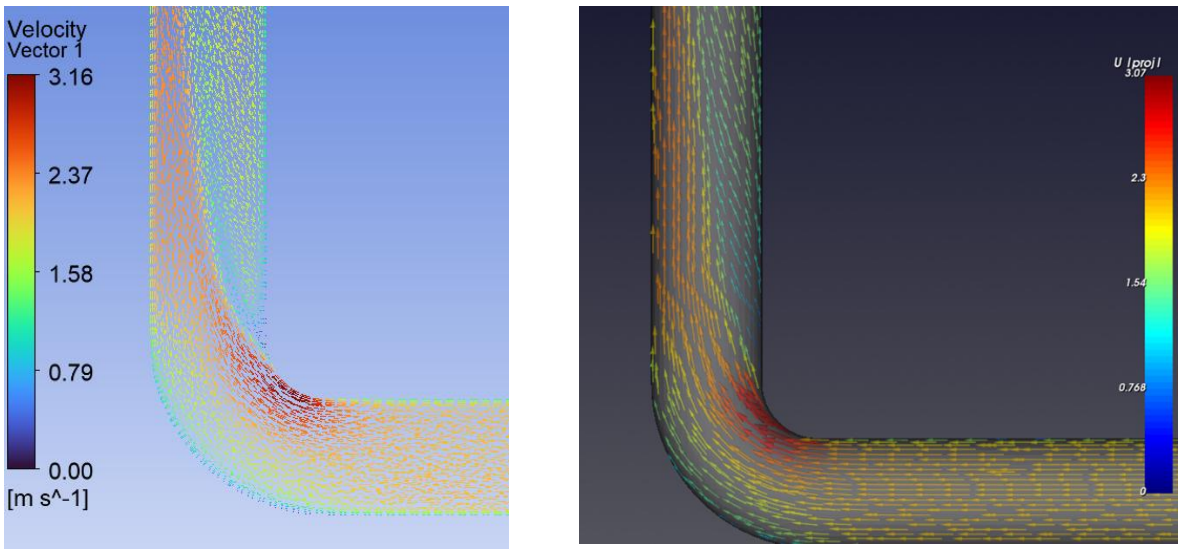

Figure 4. Velocity vector plots near the pipe bend obtained with Fluent (left) and CFxD (right).

The comparison of the U-velocity profile at 2 m downstream of the bend is shown in Figure 5.

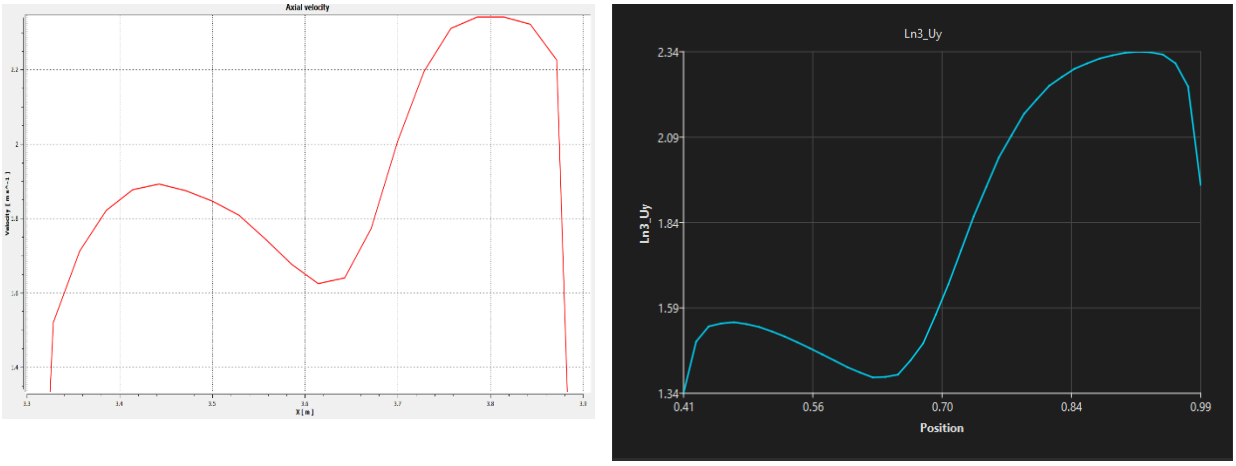

Figure 5. U-velocity profile at 2 m downstream of the bend obtained with Fluent (left) and CFxD (right).

The comparison of the U-velocity profile at 4 m downstream of the bend is shown in Figure 6.

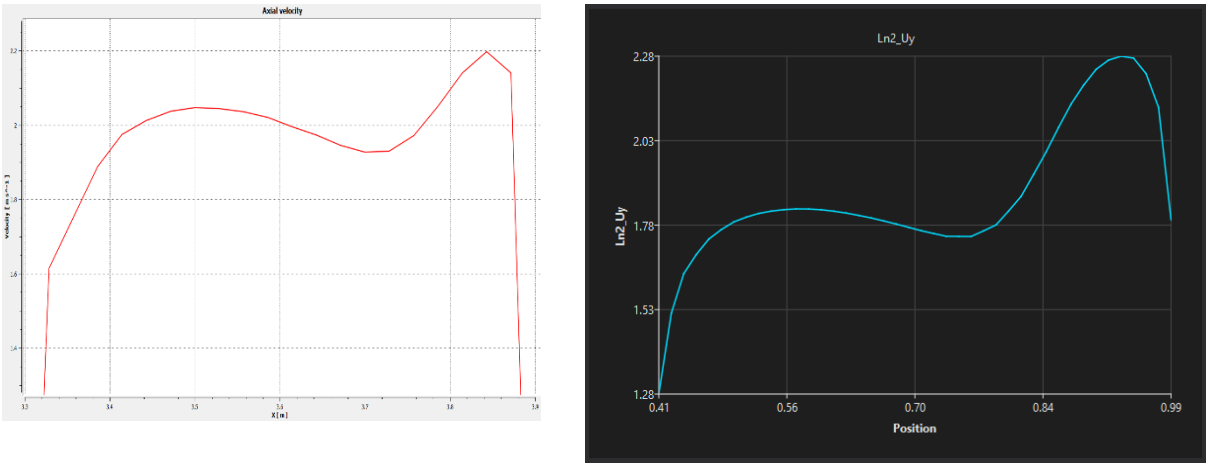

Figure 6. U-velocity profile at 4 m downstream of the bend obtained with Fluent (left) and CFxD (right).

The comparison of the U-velocity profile at 6 m downstream of the bend is shown in Figure 7.

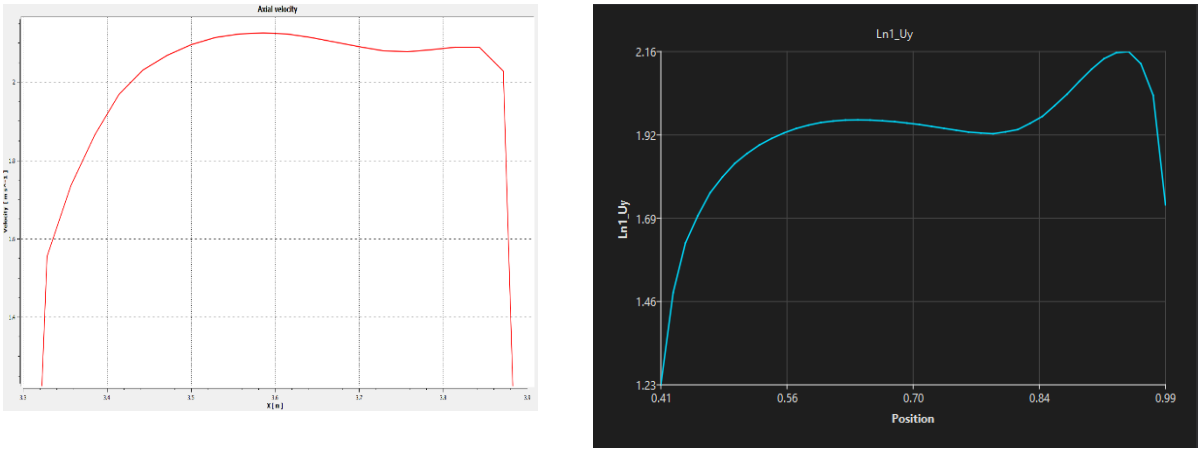

Figure 7. U-velocity profile at 6 m downstream of the bend obtained with Fluent (left) and CFxD (right).

The pressure drop predicted by Fluent is 1.33 Pa, while the value predicted by CFxD is 1.39 Pa. The relative difference is approximately 4.5%.

Conclusion

The comparison demonstrates good agreement between the CFxD and Fluent results for the incompressible turbulent flow in the pipe bend. Both simulations predict similar velocity distribution, flow acceleration through the bend, downstream recovery of the velocity profile, and comparable turbulence-field behavior. The contour plots and profile comparisons show that the main flow structures are captured consistently by both software packages.

The pressure drop predicted by Fluent is 1.33 Pa, while the pressure drop predicted by CFxD is 1.39 Pa. The difference between the two results is approximately 4.5%, which is considered acceptable for this preliminary benchmark comparison, especially considering the differences in mesh type and mesh resolution between the two simulations.

Overall, the results indicate that CFxD provides a consistent prediction for this internal incompressible turbulent-flow case under the tested mesh and solver settings.

2. Flow around a car (incompressible external flow)

The configuration represents the external aerodynamic flow around a car moving at 200 km/h, corresponding to approximately 55 m/s. The computational domain surrounding the car has dimensions of 15 m x 5 m x 5 m. Due to geometric symmetry, only half of the model is included in the computational domain.

The mesh size used for CFxD is approximately 174 thousand cells, while the mesh size used in Fluent is approximately 175 thousand cells. The SST turbulence model is used for both simulations.

Results and comparison

The velocity magnitude contour at 0.5 m from ground obtained with Fluent and CFxD is shown in Figure 8.

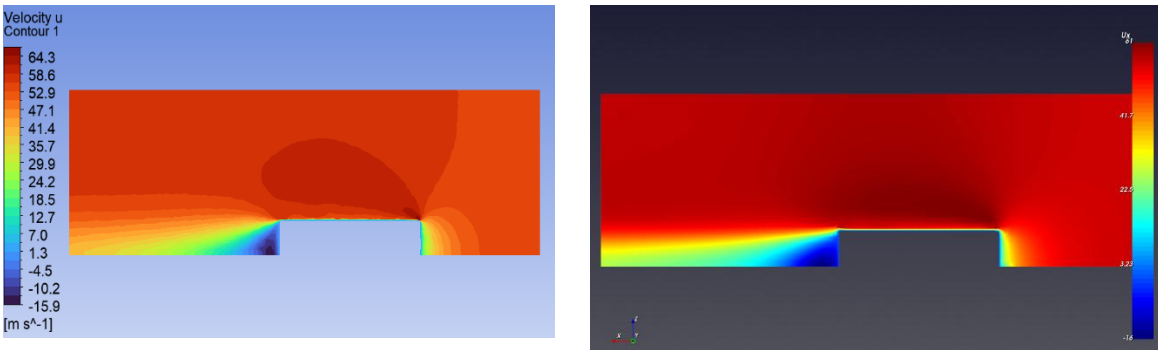

Figure 8. Velocity magnitude contour at 0.5 m from ground obtained with Fluent (left) and CFxD (right).

The velocity magnitude contour at the symmetry plane obtained with Fluent and CFxD is shown in Figure 9.

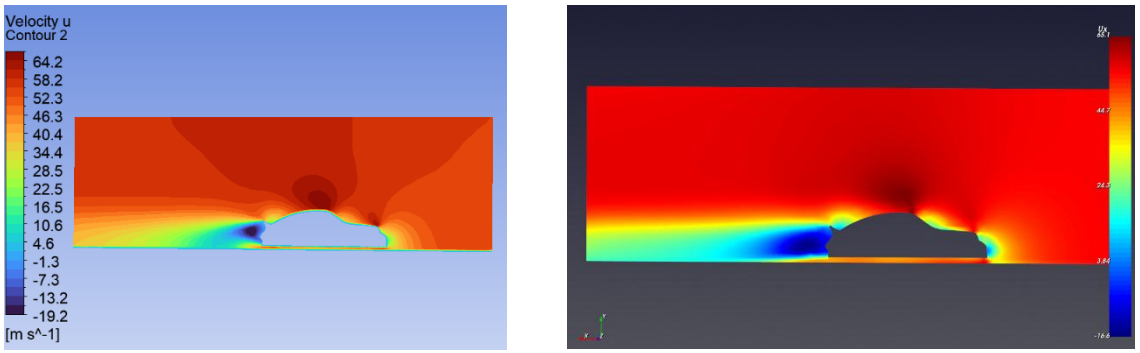

Figure 9. Velocity magnitude contour at the symmetry plane obtained with Fluent (left) and CFxD (right).

The comparison of the U-velocity profile at 3 m downstream of the car is shown in Figure 10.

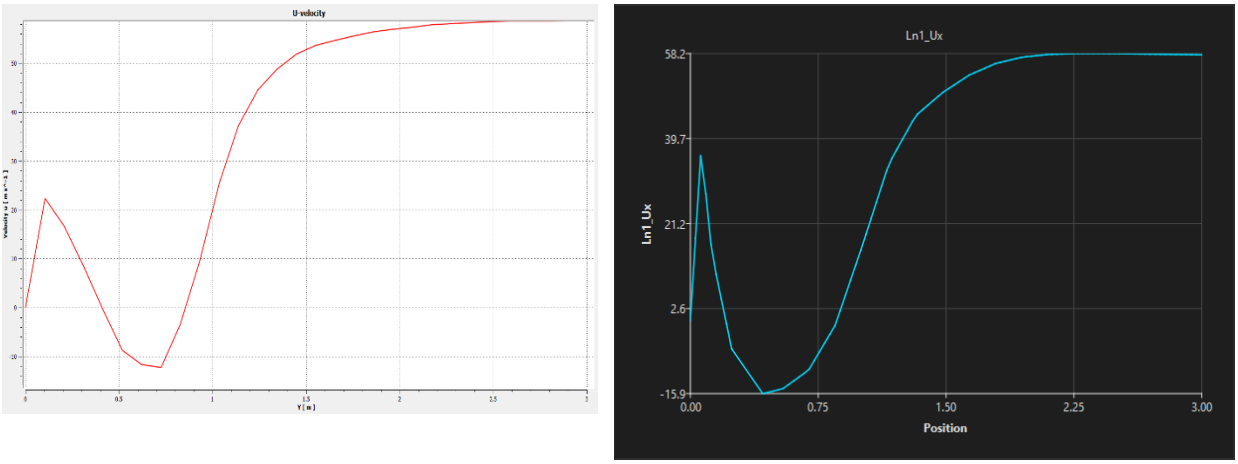

Figure 10. U-velocity profile at 3 m downstream of the car obtained with Fluent (left) and CFxD (right).

The comparison of the U-velocity profile at 4 m downstream of the car is shown in Figure 11.

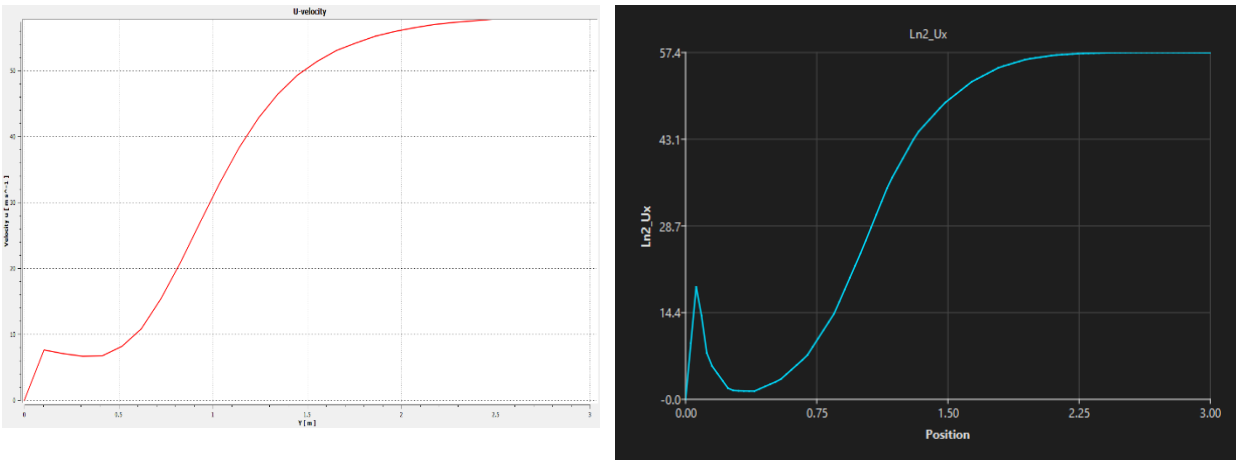

Figure 11. U-velocity profile at 4 m downstream of the car obtained with Fluent (left) and CFxD (right).

The pressure drag coefficient (Cdp) predicted by Fluent is 0.69, while the value predicted by CFxD is 0.59. The relative difference is approximately 14.6%. This difference is considered reasonable for a preliminary comparison with coarse meshes, since external vehicle aerodynamics is sensitive to near-wall resolution, wake-region discretization, and pressure integration over the vehicle surface.

Conclusion

The comparison demonstrates reasonable agreement between the CFxD and Fluent results for the external incompressible turbulent flow around the car. Both simulations predict similar acceleration of the flow around the vehicle body and a comparable wake region downstream of

the car. The velocity contours show that the main aerodynamic flow features are captured consistently by both software packages.

The U-velocity profiles at 3 m and 4 m downstream of the car show similar overall trends between the Fluent and CFxD results. The pressure drag coefficient predicted by Fluent is 0.69, while the value predicted by CFxD is 0.59, corresponding to a relative difference of approximately 14.6%. This difference is larger than in the internal pipe-flow benchmark, but it is expected to be more sensitive to mesh resolution, near-wall treatment, and wake-region discretization.

Overall, the results indicate that CFxD provides a consistent prediction for this external incompressible turbulent-flow case under the tested coarse-mesh settings.

3. Flow in a duct with heated rods (flow with heat transfer)

This case models airflow through a rectangular duct with three heated rods. The duct dimensions are 100 mm (height) × 500 mm (width) × 1500 mm (length). The inlet velocity is 2 m/s, the inlet air temperature is 288 K, and air is used as the working fluid. Symmetry conditions are applied to the top and bottom surfaces, while the remaining duct wall surfaces are maintained at 350 K. The rod surface temperature is 500 K.

The mesh size used for CFxD is approximately 134 thousand cells, while the mesh size used in Fluent is approximately 200 thousand cells. The SST turbulence model is used for both simulations.

Results and comparison

The velocity magnitude contour at the duct mid-height plane obtained with Fluent and CFxD is shown in Figure 12.

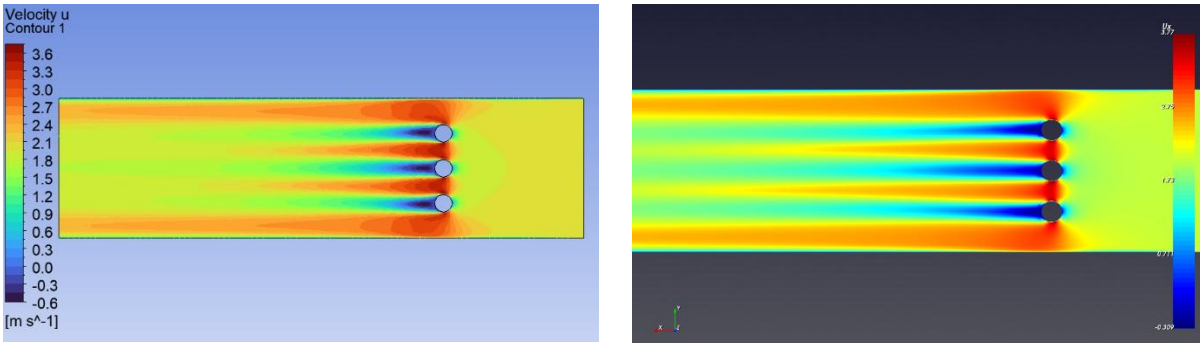

Figure 12. Velocity magnitude contour at the duct mid-height plane obtained with Fluent (left) and CFxD (right).

The temperature contour at the duct mid-height plane obtained with Fluent and CFxD is shown in Figure 13.

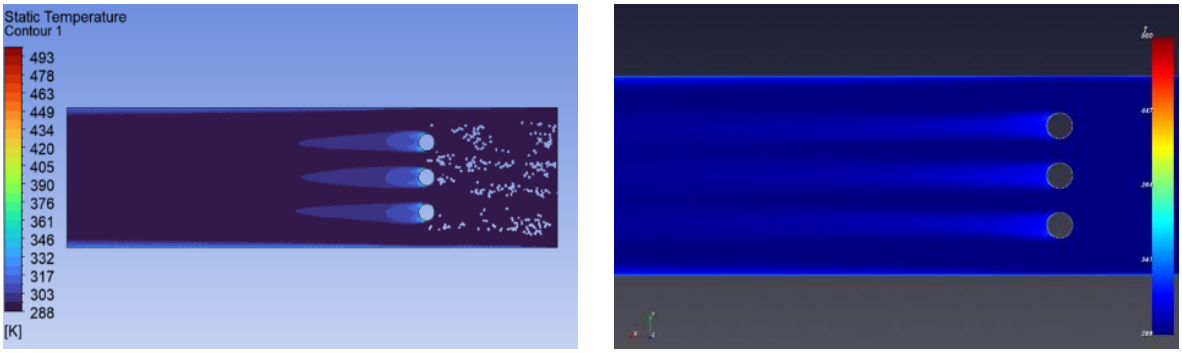

Figure 13. Temperature contour at the duct mid-height plane obtained with Fluent (left) and CFxD (right).

The comparison of the U-velocity profile at 0.46 m downstream of the rods is shown in Figure 14.

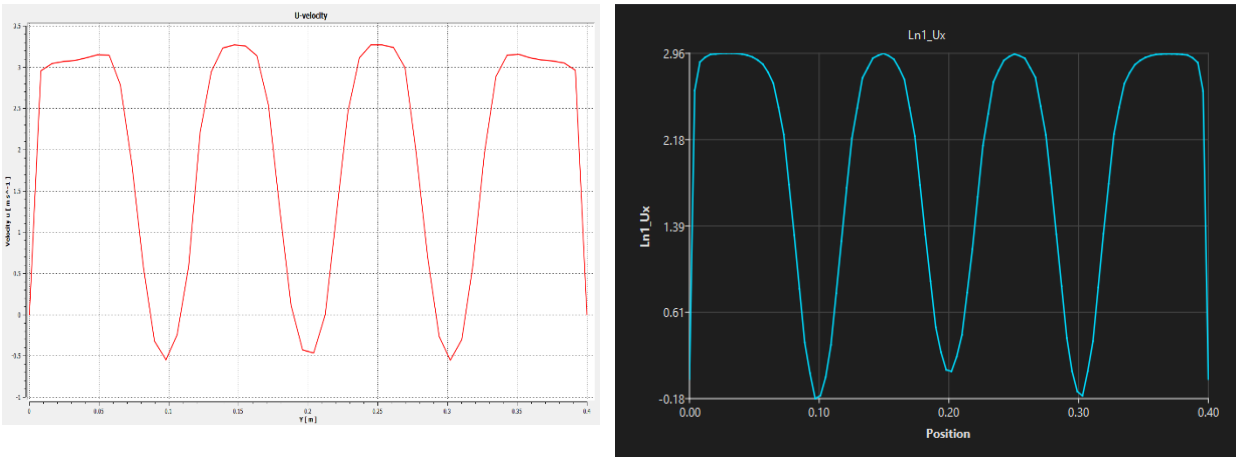

Figure 14. U-velocity profile at 0.46 m downstream of the rods obtained with Fluent (left) and CFxD (right).

The comparison of the temperature profile at 0.46 m downstream of the rods is shown in Figure 15.

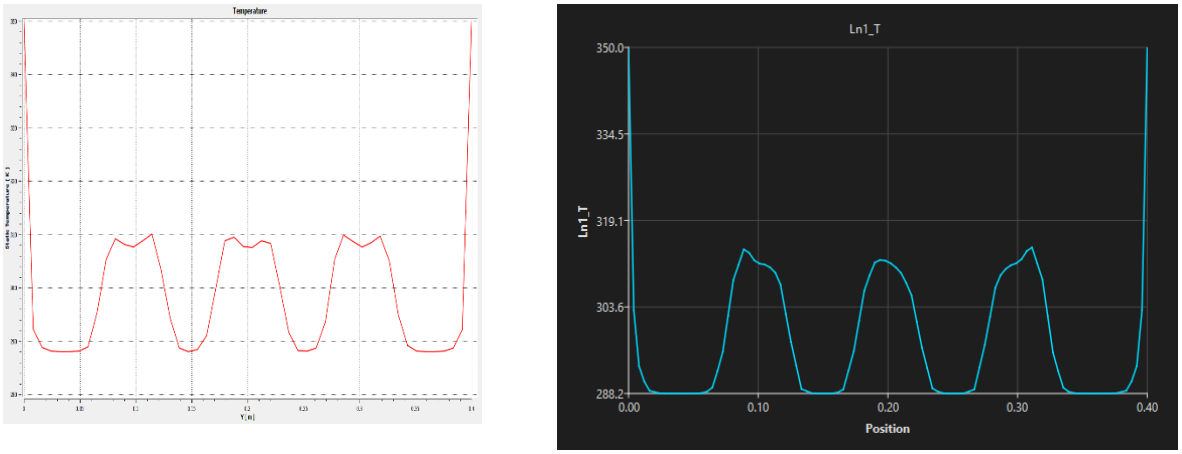

Figure 15. Temperature profile at 0.46 m downstream of the rods obtained with Fluent (left) and CFxD (right).

The outlet averaged temperature predicted by Fluent is 293.9 K, while the value predicted by CFxD is 293.4 K. The relative difference is approximately 0.17%.

Conclusion

The comparison demonstrates good agreement between the CFxD and Fluent results for airflow through the duct with heated rods. Both simulations predict similar acceleration of the flow around the rods and comparable wake behavior downstream of the heated elements. The velocity contours and U-velocity profile show that the main flow structures are captured consistently by both software packages.

The temperature contour and temperature profile also show similar overall behavior between the Fluent and CFxD results. The outlet average temperature predicted by Fluent is 293.9 K, while CFxD predicts 293.4 K, corresponding to a relative difference of approximately 0.17%. This indicates close agreement for the overall heat-transfer prediction in this benchmark case.

Overall, the results indicate that CFxD provides a consistent prediction for this forced-convection heat-transfer case under the tested mesh and solver settings.

4. Natural convection in a closed box (buoyancy-driven flow)

This case models natural convection in a closed box. The box dimensions are 200 mm in height, 500 mm in width, and 500 mm in length. A rectangular heat source is located at the center of the box floor and is maintained at a temperature of 450 K. The heat source dimensions are 10 mm in height, 50 mm in width, and 50 mm in length. The box walls are maintained at a temperature of 288 K.

The mesh size used for CFxD is approximately 243 thousand cells, while the mesh size used in Fluent is approximately 205 thousand cells. The SST model is used for both simulations.

Results and comparison

The velocity magnitude contour at the mid-plane of the box obtained with Fluent and CFxD is shown in Figure 16.

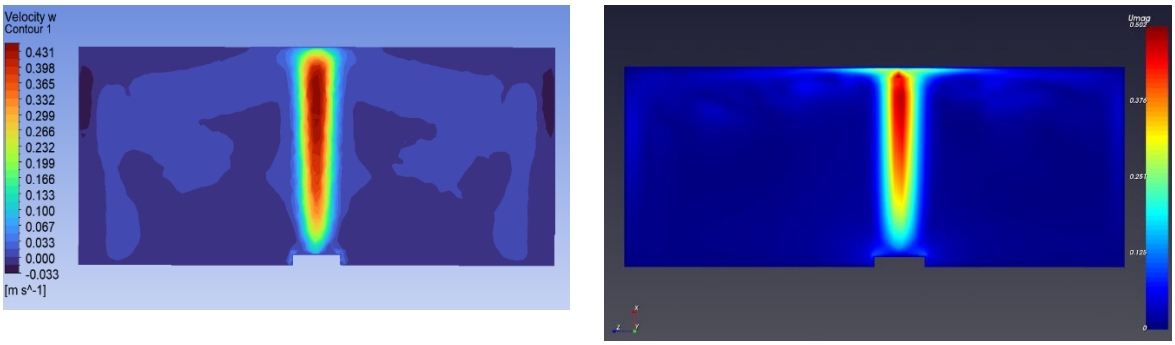

Figure 16. Velocity magnitude contour at the mid-plane of the box obtained with Fluent (left) and CFxD (right).

The temperature contour at the mid-plane of the box obtained with Fluent and CFxD is shown in Figure 17.

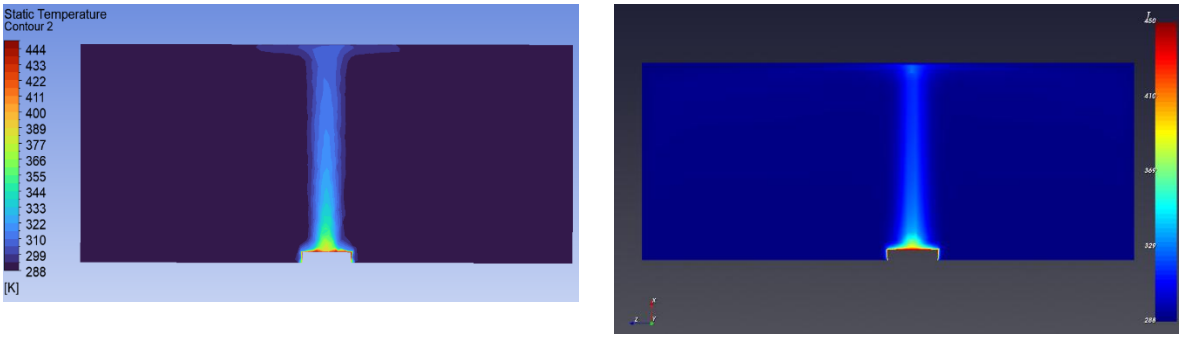

Figure 17. Temperature contour at the mid-plane plane of the box obtained with Fluent (left) and CFxD (right).

The comparison of the U-velocity profile at 0.050 m above heat source is shown in Figure 18.

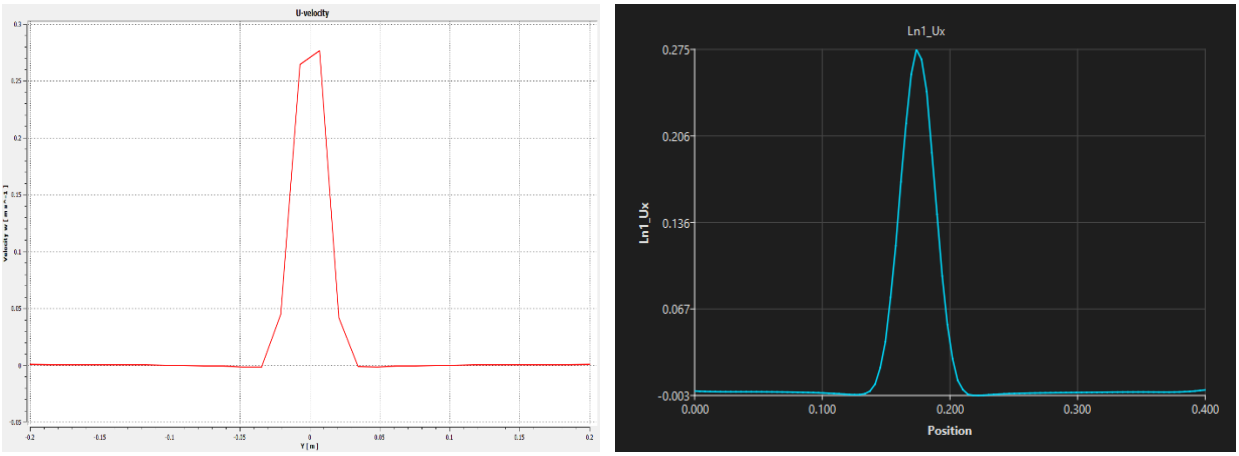

Figure 18. U-velocity profile at 0.050 m above heat source obtained with Fluent (left) and CFxD (right).

The comparison of the temperature profile at 0.050 m above heat source is shown in Figure 19.

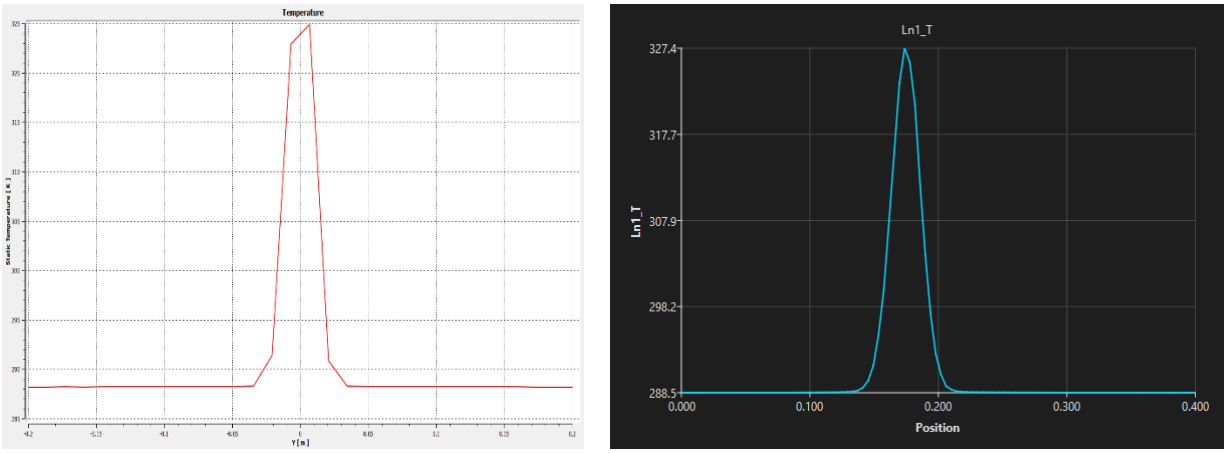

Figure 19. Temperature profile at 0.050 m above heat source obtained with Fluent (left) and CFxD (right).

The comparison of the U-velocity profile at 0.100 m above heat source is shown in Figure 20.

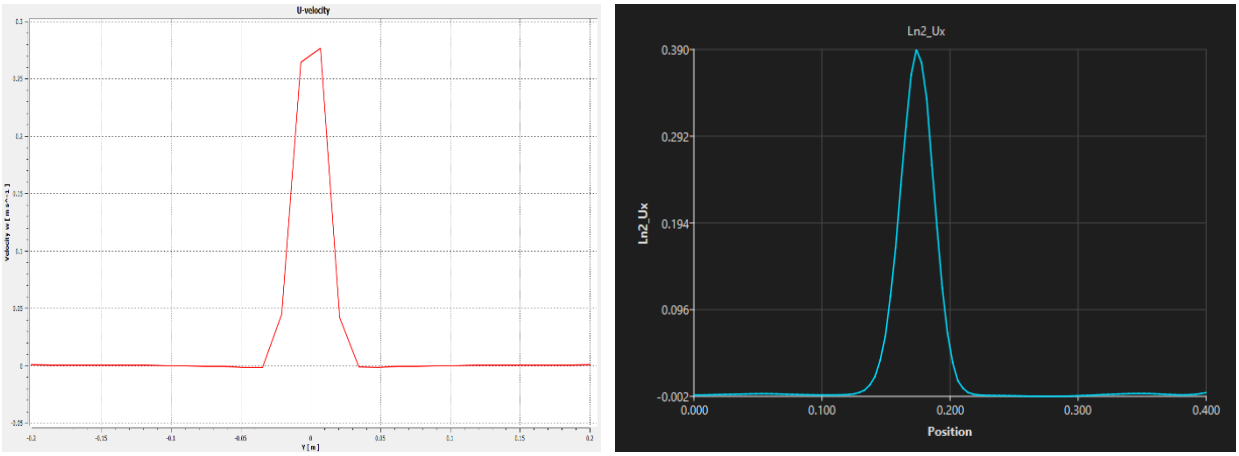

Figure 20. U-velocity profile at 0.100 m above heat source obtained with Fluent (left) and CFxD (right).

The comparison of the temperature profile at 0.100 m above heat source is shown in Figure 21.

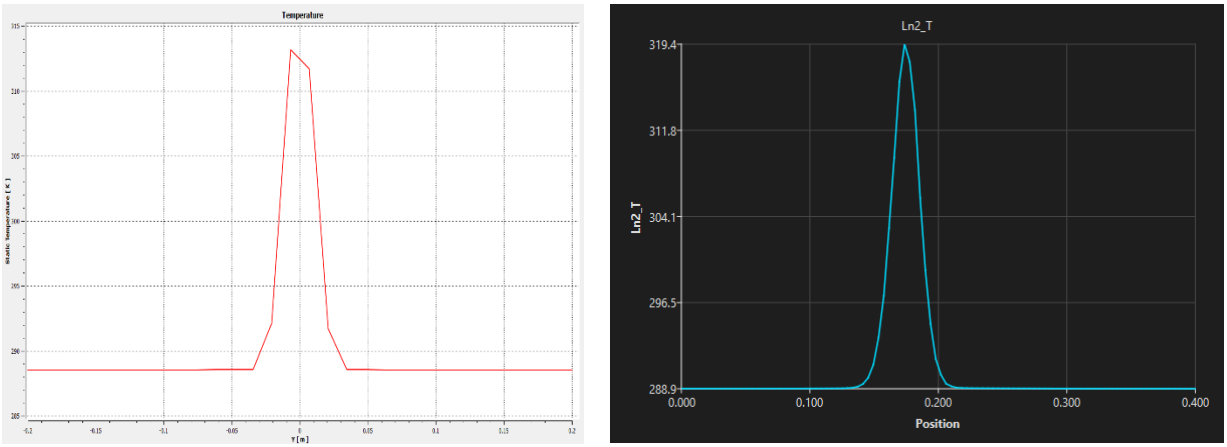

Figure 21. Temperature profile at 0.100 m above heat source obtained with Fluent (left) and CFxD (right).

Conclusion

The comparison demonstrates reasonable agreement between the CFxD and Fluent results for buoyancy-driven flow in the closed box. Both simulations predict the development of an upward thermal plume above the heated source and recirculating flow within the enclosure. The velocity and temperature contours show that the main natural-convection flow structures are captured consistently by both software packages.

The velocity and temperature profiles at 0.050 m and 0.100 m above the heat source show similar overall trends between the Fluent and CFxD results. Differences between the two predictions are expected because the meshes are not identical and the solution is sensitive to the near-wall thermal boundary layers, buoyancy treatment, and turbulence-model selection.

Overall, the results indicate that CFxD provides a consistent prediction for this closed-box buoyancy-driven heat-transfer case under the tested mesh and solver settings.

5. Free jet in open air (compressible subsonic flow, M<1)

This case represents a free round jet with a diameter D = 1.0 m discharging into open air. The jet exit velocity is 300 m/s, while the surrounding (co-flow) air velocity is 10 m/s. The jet temperature is 700 K and the surrounding air temperature is 288.15 K (standard ambient). The jet Mach number is 0.57.

The mesh size used for CFxD is approximately 99 thousand cells, while the mesh size used in Fluent is approximately 98 thousand cells. The k-epsilon turbulence model is used for both simulations. Compressible flow and heat transfer are included in both simulations.

Results and comparison

The velocity magnitude contour at the symmetry plane obtained with Fluent and CFxD is shown in Figure 22.

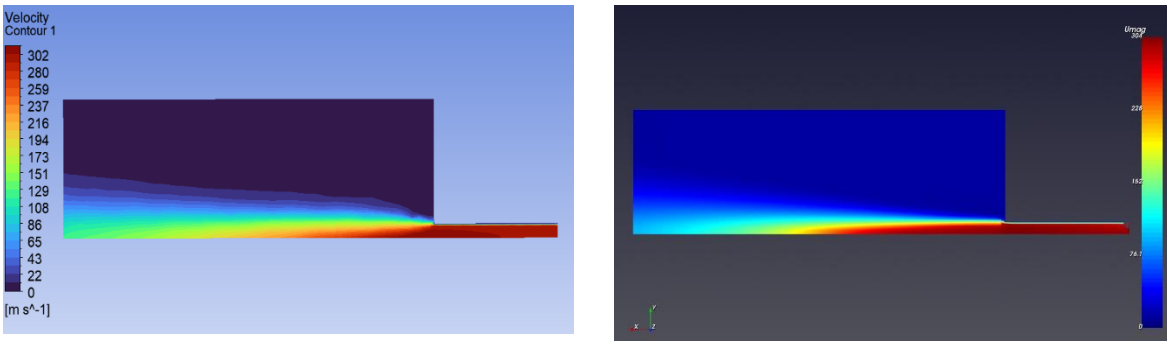

Figure 22. Velocity magnitude contour at the symmetry plane obtained with Fluent (left) and CFxD (right).

The temperature contour at the symmetry plane obtained with Fluent and CFxD is shown in Figure 23.

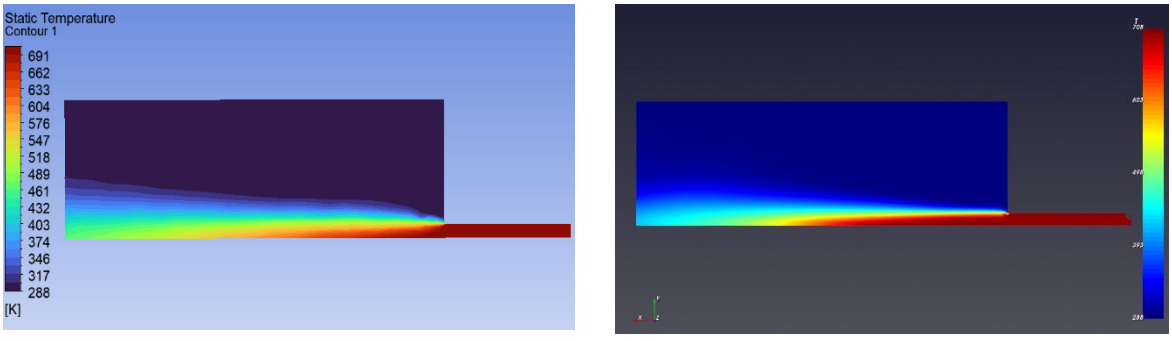

Figure 23. Temperature contour at the symmetry plane obtained with Fluent (left) and CFxD (right).

The comparison of the U-velocity profile at 5 m downstream of the jet exit is shown in Figure 24.

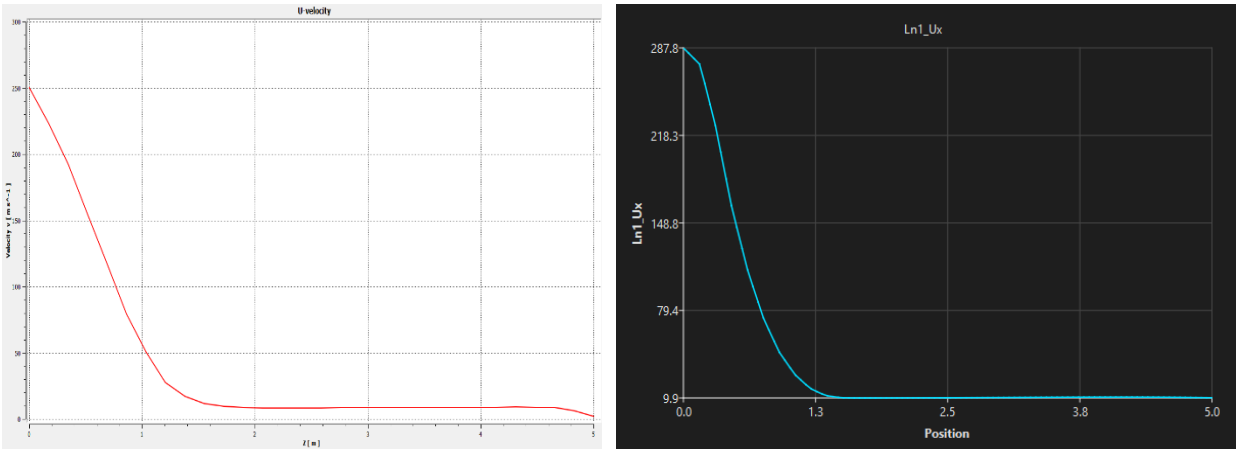

Figure 24. U-velocity profile at 5 m downstream of the jet exit obtained with Fluent (left) and CFxD (right).

The comparison of the temperature profile at 5 m downstream of the jet exit is shown in Figure 25.

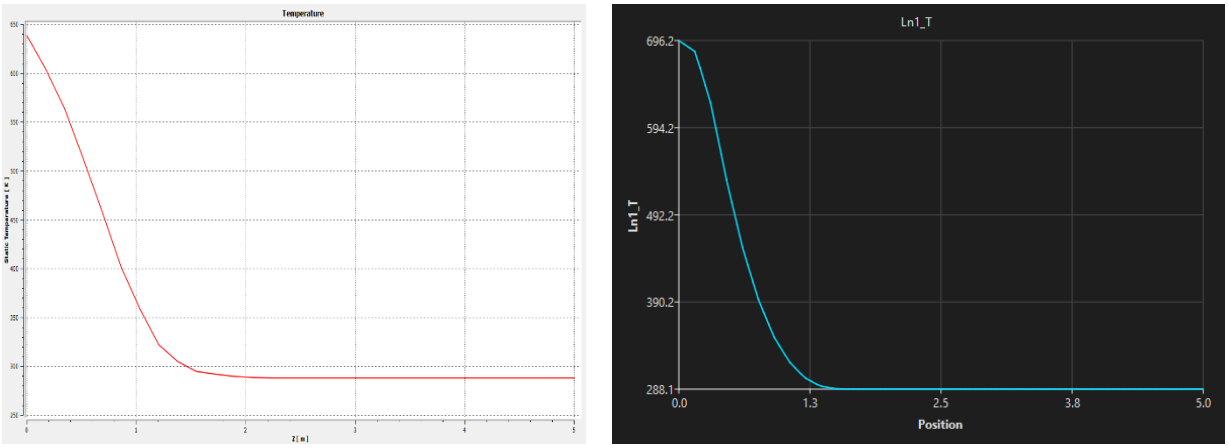

Figure 25. Temperature profile at 5 m downstream of the jet exit obtained with Fluent (left) and CFxD (right).

The comparison of the U-velocity profile at 10 m downstream of the jet exit is shown in Figure 26.

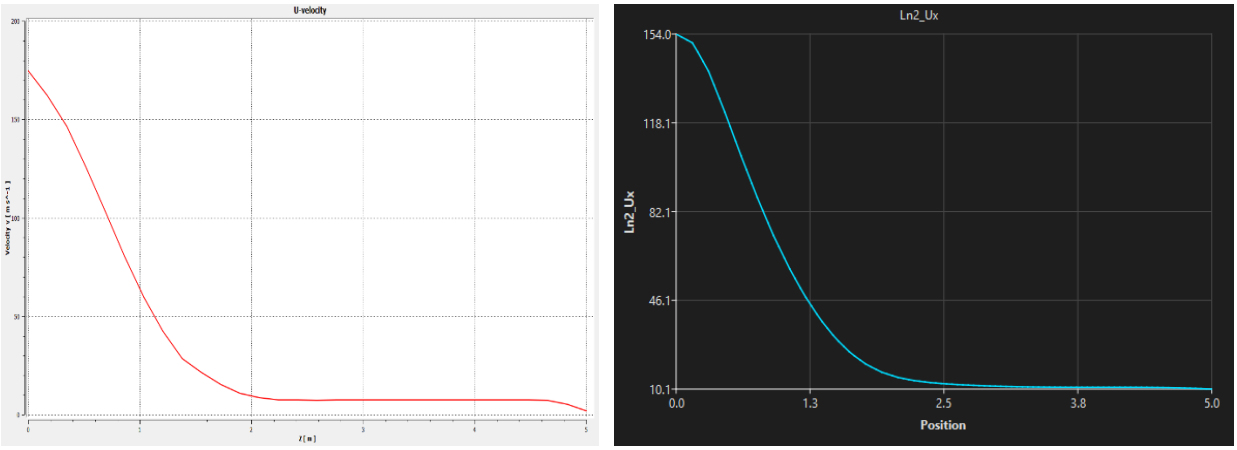

Figure 26. U-velocity profile at 10 m downstream of the jet exit obtained with Fluent (left) and CFxD (right).

The comparison of the temperature profile at 10 m downstream of the jet exit is shown in Figure 27.

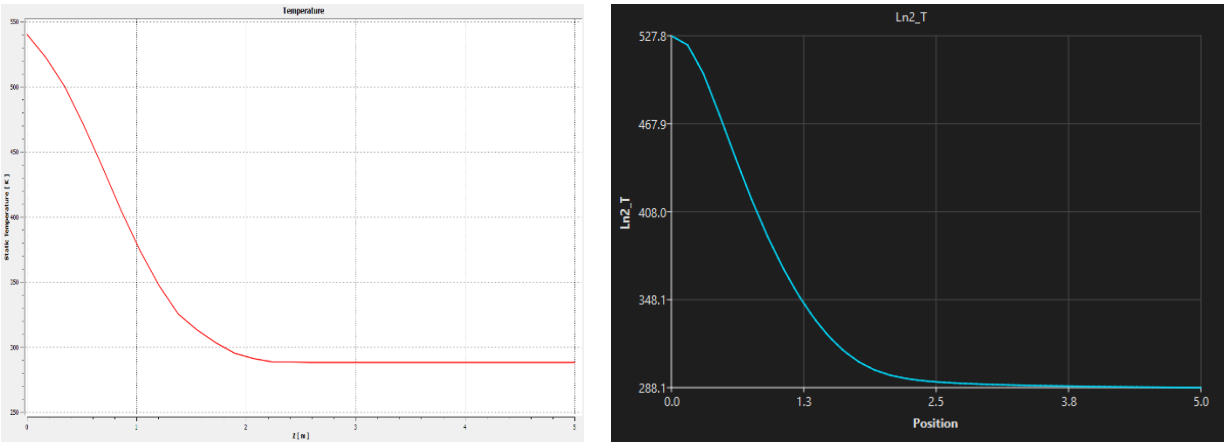

Figure 27. Temperature profile at 10 m downstream of the jet exit obtained with Fluent (left) and CFxD (right).

Conclusion

The comparison demonstrates reasonable agreement between the CFxD and Fluent results for the compressible subsonic free jet. Both simulations predict a high-velocity jet core near the outlet, followed by jet spreading, entrainment of the surrounding air, and gradual decay of the centerline velocity. The velocity and temperature contours show that the principal jet-flow structures are captured consistently by both software packages.

The velocity and temperature profiles at 5 m and 10 m downstream of the jet exit show similar overall trends between the Fluent and CFxD results. Both simulations predict progressive broadening of the jet and reduction of the peak velocity and temperature with increasing

downstream distance. Differences between the two predictions may result from variations in mesh structure, numerical diffusion, turbulence-model implementation, and treatment of the open boundaries.

Overall, the results indicate that CFxD provides a consistent prediction for this compressible subsonic jet-flow case under the tested mesh and solver settings.

6. Flow in a pipe with a butterfly valve (thin internal wall)

This case represents flow through a cylindrical pipe with a diameter D = 1.0 m. A butterfly valve is positioned inside the pipe at an angle of 45°. The inlet velocity is 5 m/s, and air is used as the working fluid.

The mesh size used for CFxD is approximately 128 thousand cells, while the mesh size used in Fluent is approximately 121 thousand cells. The k-epsilon turbulence model is used for both simulations.

Results and comparison

The velocity magnitude contour at the symmetry plane obtained with Fluent and CFxD is shown in Figure 28.

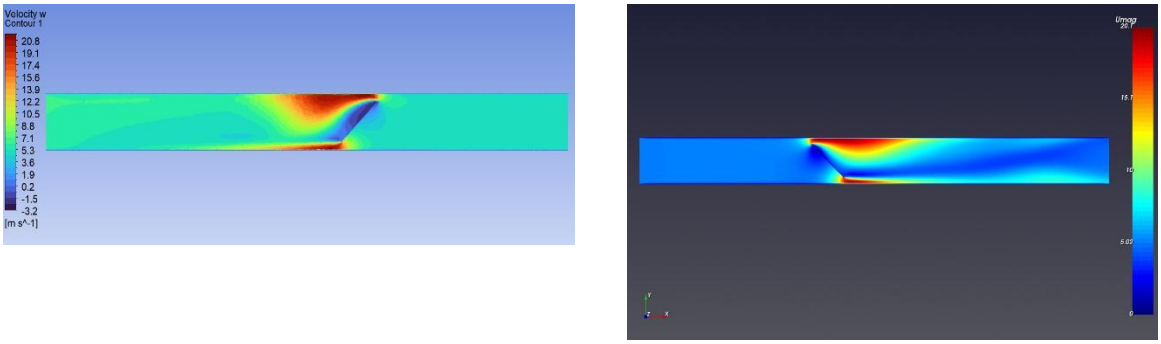

Figure 28. Velocity magnitude contour at the symmetry plane obtained with Fluent (left) and CFxD (right).

The gauge pressure contour at the symmetry plane obtained with Fluent and CFxD is shown in Figure 29.

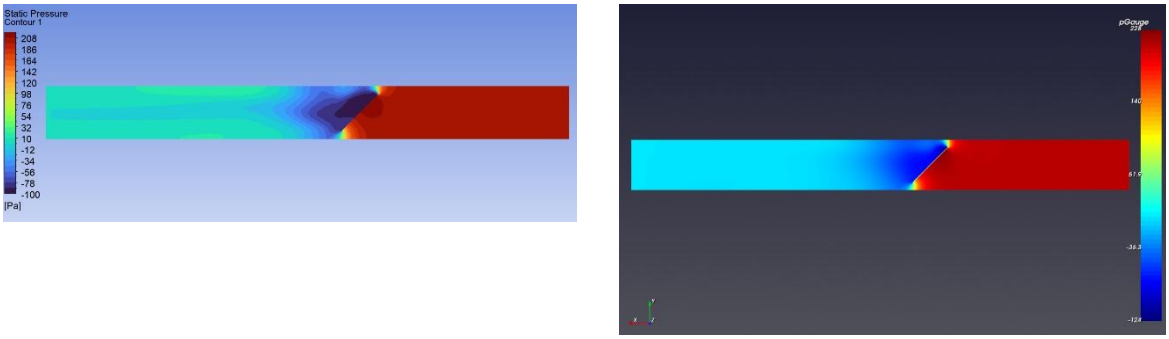

Figure 29. Gauge pressure contour at the symmetry plane obtained with Fluent (left) and CFxD (right).

The comparison of the U-velocity profile at 5 m downstream of the inlet is shown in Figure 30.

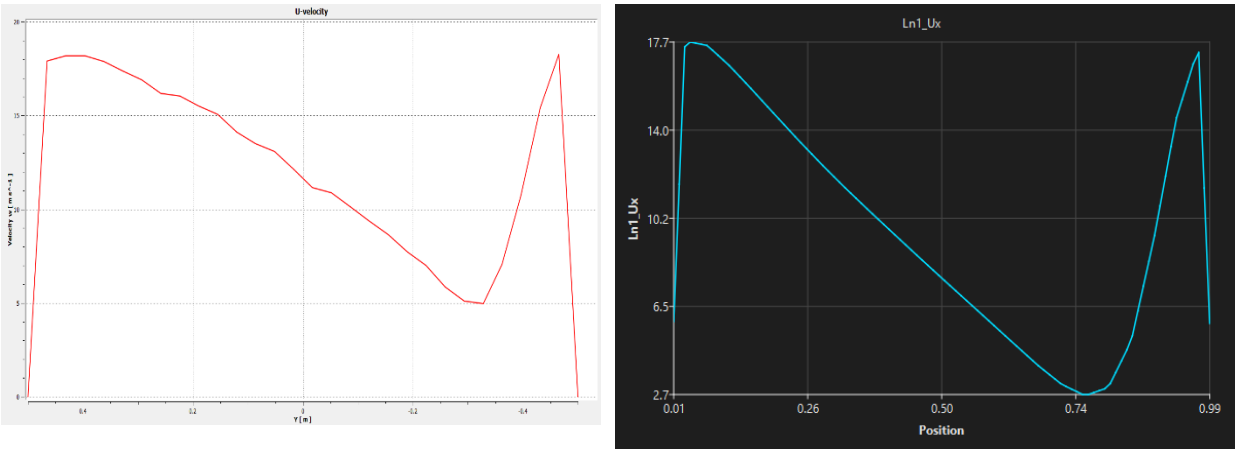

Figure 30. U-velocity profile at 5 m downstream of the inlet obtained with Fluent (left) and CFxD (right).

The comparison of the U-velocity profile at 6 m downstream of the inlet is shown in Figure 31.

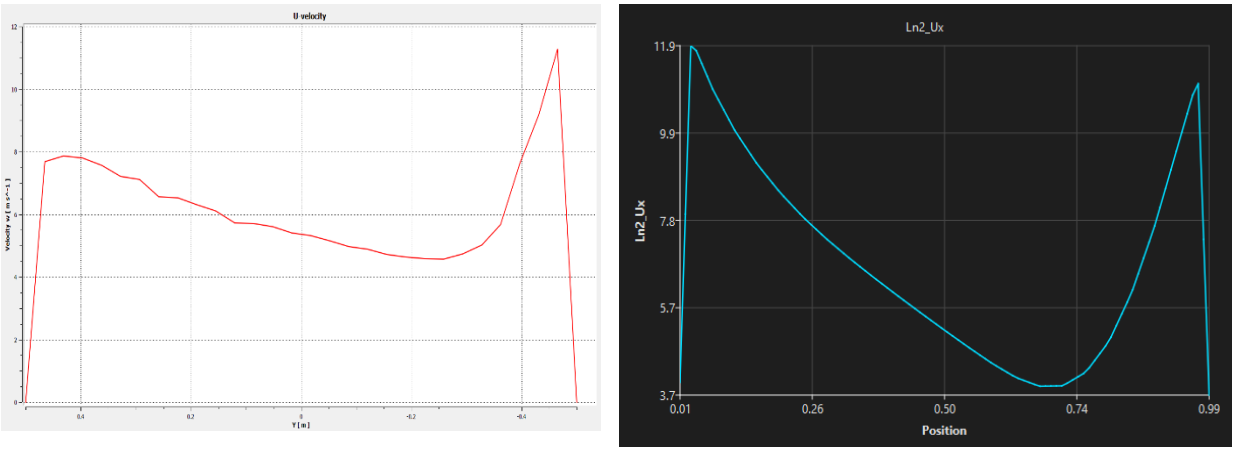

Figure 31. U-velocity profile at 6 m downstream of the inlet obtained with Fluent (left) and CFxD (right).

The pressure drop predicted by Fluent is 204 Pa, while the value predicted by CFxD is 224 Pa. The relative difference is approximately 9.8%.

Conclusion

The comparison demonstrates reasonable agreement between the CFxD and Fluent results for turbulent airflow through the pipe with a partially closed butterfly valve. Both simulations predict strong flow acceleration through the restricted opening, a corresponding pressure decrease across the valve, and a disturbed wake region downstream of the valve. The velocity and pressure contours show that the principal flow structures are captured consistently by both software packages.

The U-velocity profiles at 5 m and 6 m downstream of the inlet show similar overall trends between the Fluent and CFxD results. The pressure drop predicted by Fluent is 204 Pa, while CFxD predicts 224 Pa, corresponding to a relative difference of approximately 9.8%. The difference may be influenced by mesh resolution near the valve edge, wake-region discretization, and pressure integration across the valve.

Overall, the results indicate that CFxD provides a consistent prediction for this internal turbulent-flow case with a thin internal obstruction under the tested mesh and solver settings.

7. Flow in a settling chamber (porous media)

This case models airflow through a test rig used for aerodynamical measurements. The system consists of a pipe with a diameter D = 100 mm, a 90° bend, a diffuser, and a settling chamber with a diameter of D = 300 mm. The pressure loss coefficients are ζ = 3 for the screen and ζ = 5 for the perforated plate. The screen is represented as a porous jump with negligible thickness, while the perforated plate is represented as a porous zone with a thickness of 50 mm. The inlet velocity is 10 m/s, and air is used as the working fluid.

The mesh size used for CFxD is approximately 101 thousand cells, while the mesh size used in Fluent is approximately 115 thousand cells. The k-epsilon turbulence model is used for both simulations.

Results and comparison

The velocity magnitude contour at the symmetry plane obtained with Fluent and CFxD is shown in Figure 32.

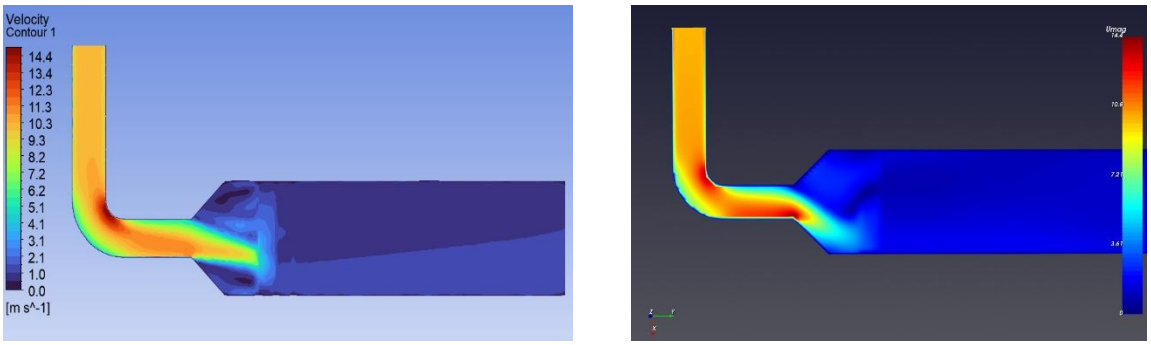

Figure 32. Velocity magnitude contour at the symmetry plane obtained with Fluent (left) and CFxD (right).

The gauge pressure contour at the symmetry plane obtained with Fluent and CFxD is shown in Figure 33.

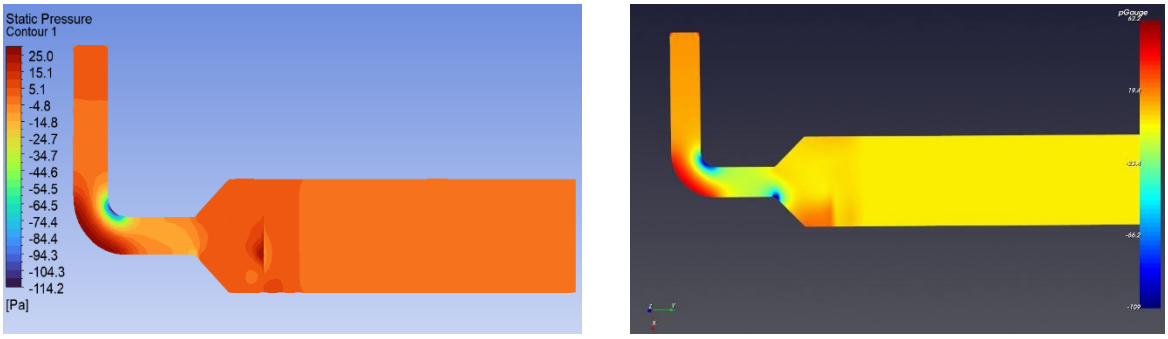

Figure 33. Gauge pressure contour at the symmetry plane obtained with Fluent (left) and CFxD (right).

The comparison of the V-velocity profile at 1.4 m downstream of the bend is shown in Figure 34.

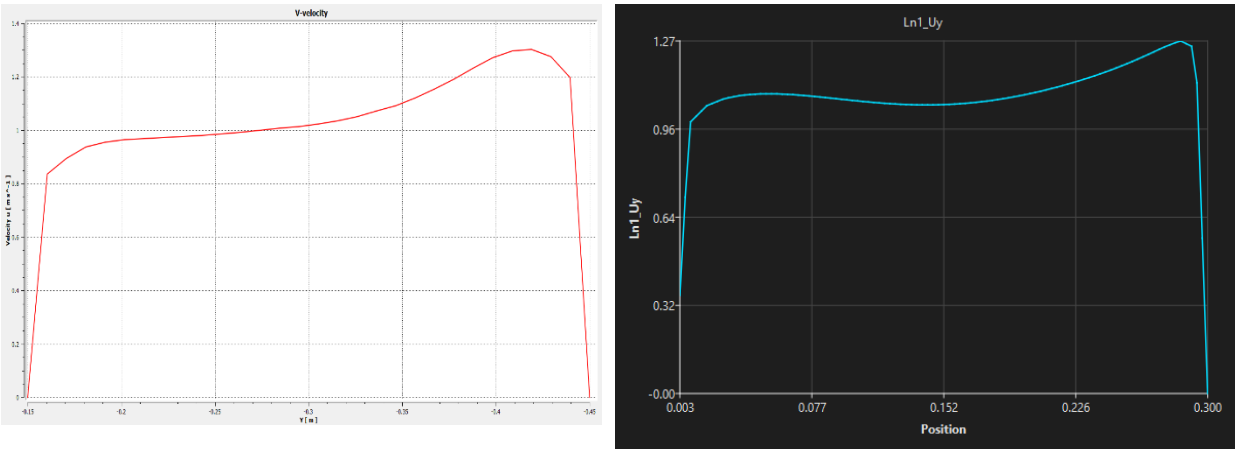

Figure 34. V-velocity profile at 1.4 m downstream of bend obtained with Fluent (left) and CFxD (right).

Conclusion

The comparison demonstrates reasonable agreement between the CFxD and Fluent results for airflow through the settling chamber with porous-resistance elements. Both simulations predict the pressure loss across the screen and perforated plate, together with a reduction in velocity non-uniformity downstream of the resistance elements. The velocity and pressure contours show that the principal flow features are captured consistently by both software packages.

The V-velocity profile at 1.4 m downstream of the bend shows a similar overall trend between the Fluent and CFxD results. Differences between the two predictions may result from variations in mesh structure, implementation of the porous-resistance model, and local flow resolution through the diffuser and settling chamber.

Overall, the results indicate that CFxD provides a consistent prediction for this turbulent porous-media flow case under the tested mesh and solver settings.

8. Transient flow around a cylinder (laminar vortex shedding)

This case models transient airflow around a circular cylinder and the resulting periodic vortex shedding. The cylinder diameter is D = 10 mm, and the inlet velocity is U = 1.30 m/s. For air, the Reynolds number based on the cylinder diameter and inlet velocity is approximately Re = 800. The laminar flow model is used for both simulations. A time step of 0.001 s is used, and the total simulated time is 0.6 s.

The mesh used in CFxD contains approximately 159 thousand cells. An initially coarser Fluent mesh did not reproduce the same periodic wake behavior because the cylinder boundary layer and downstream vortex structures were insufficiently resolved. Therefore, the Fluent mesh was refined to approximately 828 thousand cells to obtain a developed vortex-shedding pattern. Consequently, this case should be interpreted primarily as a qualitative comparison of the transient wake structures rather than a mesh-equivalent quantitative verification.

Results and comparison

The instantaneous velocity magnitude contours obtained with Fluent and CFxD are shown in Figure 35.

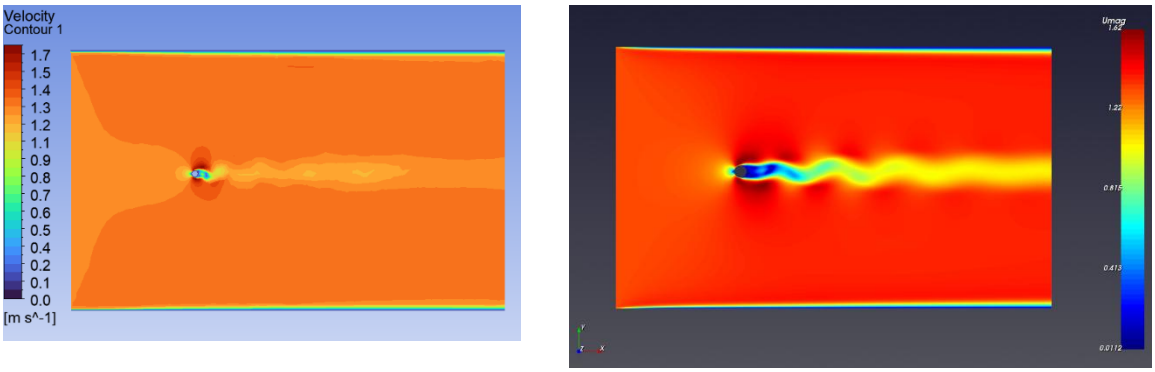

Figure 35. Instantaneous velocity magnitude contours showing vortex shedding downstream of the cylinder, obtained with Fluent (left) and CFxD (right).

Conclusion

Both CFxD and Fluent predict an unsteady wake downstream of the cylinder, with alternating vortical structures associated with periodic vortex shedding. The instantaneous velocity contours show that the principal transient wake behavior is reproduced by both software packages.

The Fluent simulation required a substantially finer mesh than the CFxD simulation to reproduce a comparable unsteady wake pattern. With a coarse Fluent mesh, numerical diffusion and insufficient resolution near the cylinder and in the wake suppressed or weakened the periodic vortex-shedding behavior. The difference in mesh resolution should therefore be considered when comparing the detailed vortex size, position, and downstream dissipation.

Because vortex shedding is periodic, instantaneous contours from the two simulations do not necessarily represent the same phase of the shedding cycle. Consequently, exact correspondence between individual vortices should not be expected. A more rigorous comparison should be based on time histories of lift and drag coefficients, shedding frequency, and the corresponding Strouhal number rather than on a single instantaneous contour.

Overall, the results indicate that CFxD reproduces the principal transient-flow behavior associated with vortex shedding around a circular cylinder under the tested numerical settings.

9. Two-inlet gas mixing flow (Air + CO2)

This case models the non-reacting mixing of air and carbon dioxide in a cylindrical chamber with a central air inlet and a surrounding annular CO_2 inlet. This case models the non-reacting mixing of air and carbon dioxide in a cylindrical chamber with a central air inlet and a surrounding annular CO_2 inlet. The chamber has a diameter of D = 40 mm and a length of L = 200 mm.

The central air inlet has a diameter of D = 8 mm, an inlet velocity of U = 2.0 m/s, and an inlet temperature of T = 500 K. The surrounding CO_2 inlet is annular, with an outer diameter of 40 mm and an inner diameter corresponding to the central air inlet. The CO_2 inlet velocity is U = 1.0 m/s, and its inlet temperature is T = 300 K.

The mesh size used in CFxD is approximately 105 thousand cells, while the mesh size used in Fluent is approximately 125 thousand cells. The k-epsilon turbulence model is used for both simulations. Heat transfer and species transport are included in both simulations, and no chemical reaction is considered.

Results and comparison

The velocity magnitude contour at the symmetry plane obtained with Fluent and CFxD is shown in Figure 36.

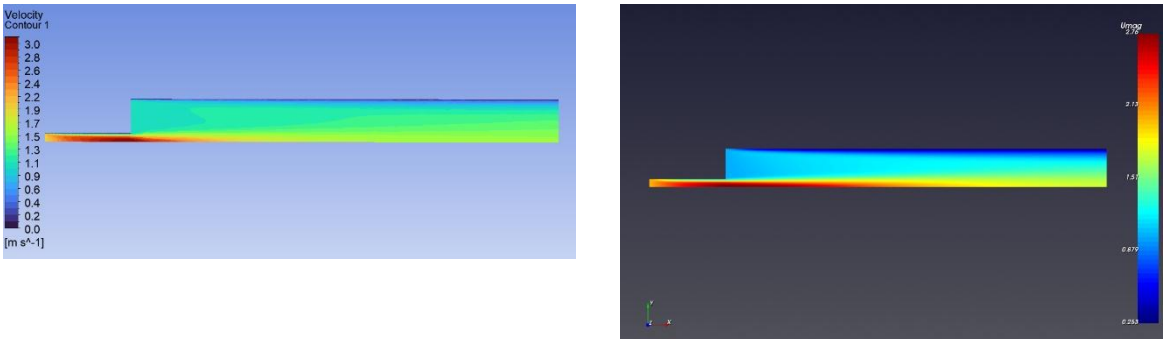

Figure 36. Velocity magnitude contour at the symmetry plane obtained with Fluent (left) and CFxD (right).

The temperature contour at the symmetry plane obtained with Fluent and CFxD is shown in Figure 37.

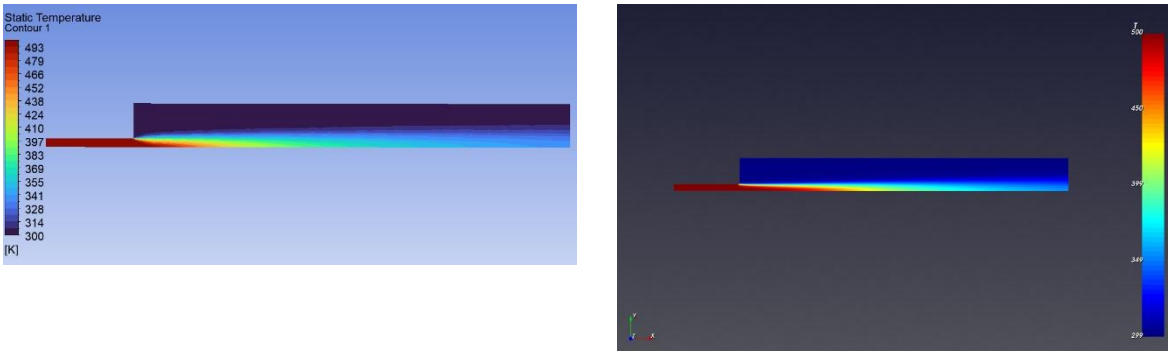

Figure 37. Temperature contour at the symmetry plane obtained with Fluent (left) and CFxD (right).

The air mass fraction contour at the symmetry plane obtained with Fluent and CFxD is shown in Figure 38.

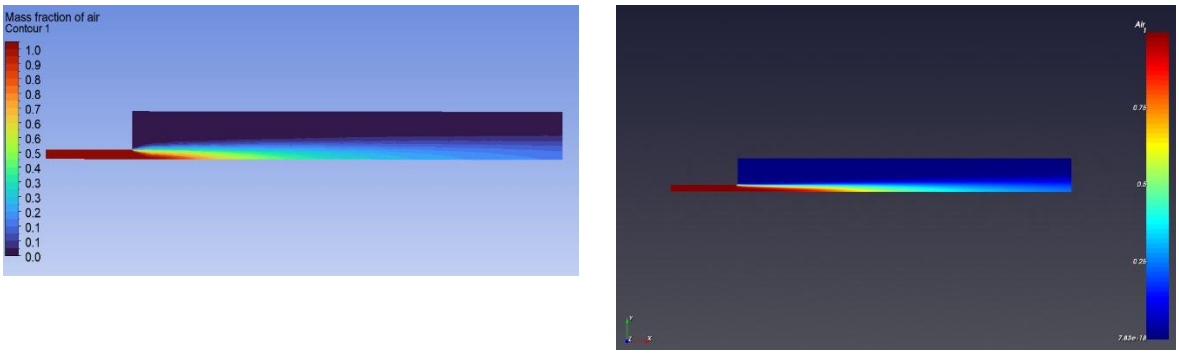

Figure 38. Air mass fraction contour at the symmetry plane obtained with Fluent (left) and CFxD (right).

The comparison of the U-velocity profile at 0.1 m downstream of the inlet plane is shown in Figure 39.

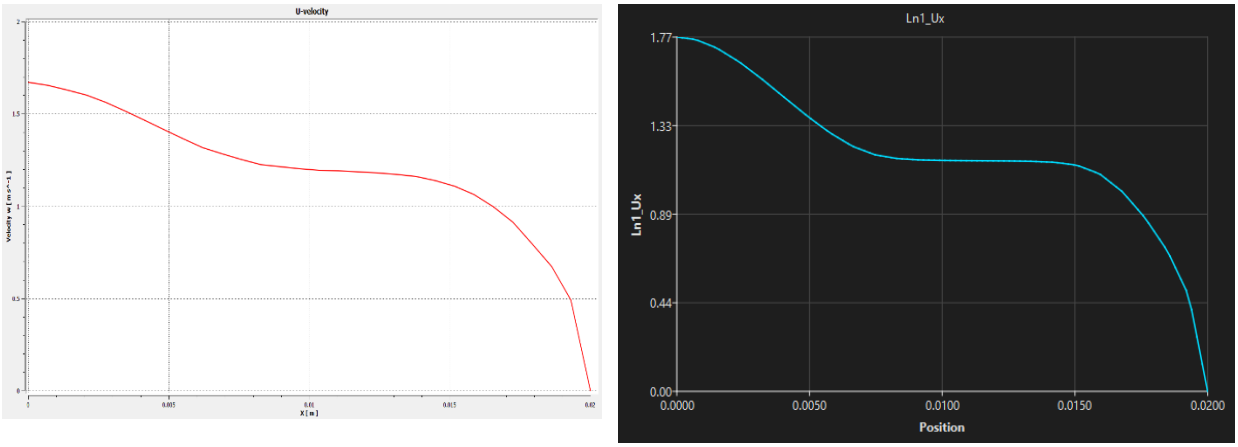

Figure 39. U-velocity profile at 0.1 m downstream of the inlet plane obtained with Fluent (left) and CFxD (right).

The comparison of the temperature profile at 0.1 m downstream of the inlet plane is shown in Figure 40.

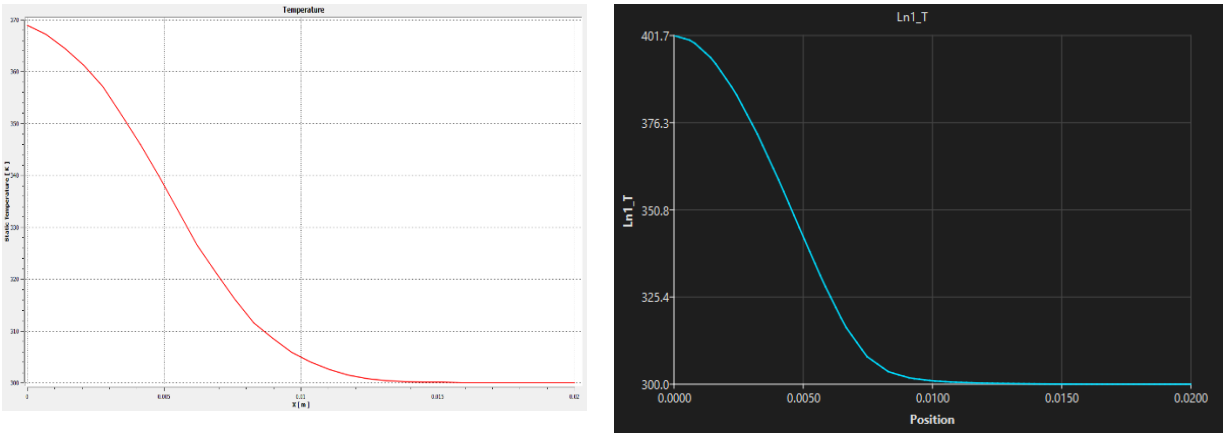

Figure 40. Temperature profile at 0.1 m downstream of the inlet plane obtained with Fluent (left) and CFxD (right).

The comparison of the air mass fraction profile at 0.1 m downstream of the inlet plane is shown in Figure 41.

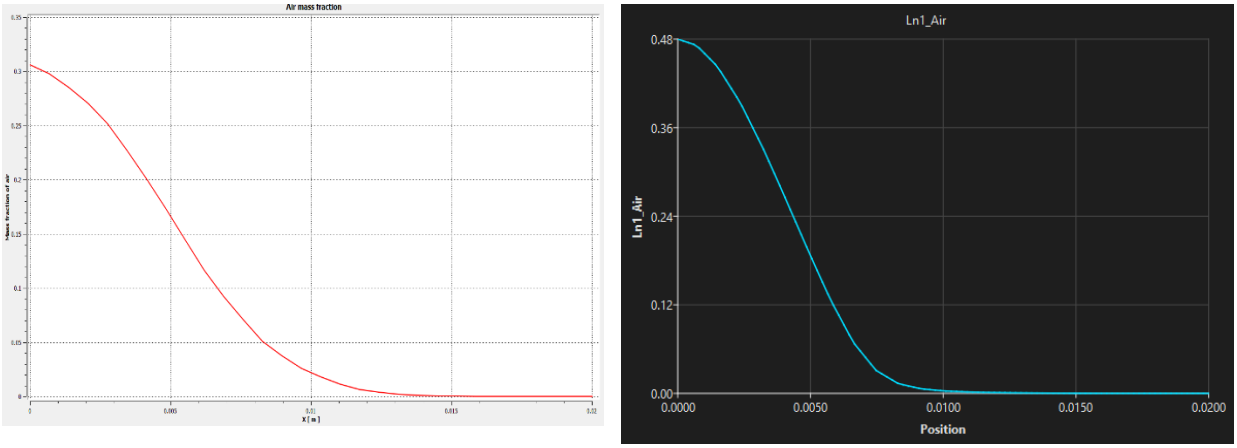

Figure 41. Air mass fraction profile at 0.1 m downstream of the inlet plane obtained with Fluent (left) and CFxD (right).

Conclusion

The comparison demonstrates reasonable agreement between the CFxD and Fluent results for the non-reacting mixing of air and carbon dioxide in the cylindrical chamber. Both simulations predict the development of a central high-temperature air stream, its interaction with the surrounding CO_2 flow, and the progressive mixing of the two gases downstream of the inlet plane.

The velocity, temperature, and air mass-fraction contours show that the principal flow and mixing structures are captured consistently by both software packages. The profiles at 0.1 m downstream of the inlet plane also show similar overall trends in velocity, temperature, and species concentration.

Differences between the two predictions may result from variations in mesh structure, numerical diffusion, turbulent species diffusivity, and the implementation of species-transport and thermophysical-property models.

Overall, the results indicate that CFxD provides a consistent prediction for this non-reacting gas-mixture flow under the tested mesh and solver settings.

Chapter II. Advanced benchmark cases

This chapter presents advanced benchmark cases covering **rotating-flow modeling (MRF)** and **conjugate heat transfer (CHT)**.

10. Flow with rotation (MRF)

This case models airflow through a cylindrical pipe containing a rotating fan. The pipe has a diameter of D = 200 mm. The fan is enclosed within a rotating reference-frame region and operates at a rotational speed of 200 rpm. The inlet velocity is 5 m/s, and air is used as the working fluid.

The mesh size used in CFxD is approximately 621 thousand cells, while the mesh size used in Fluent is approximately 828 thousand cells. The SST turbulence model and the multiple reference frame (MRF) approach is used for both simulations.

Results and comparison

The velocity magnitude contour on the YZ plane obtained with Fluent and CFxD is shown in Figure 42.

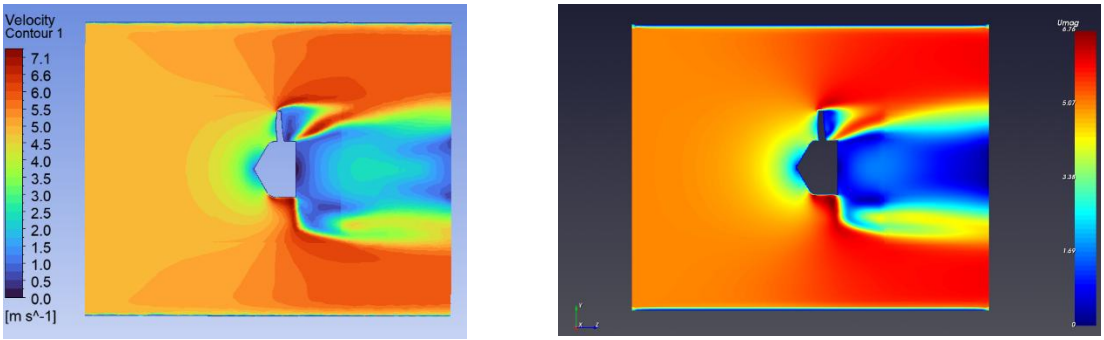

Figure 42. Velocity magnitude contour on the YZ plane obtained with Fluent (left) and CFxD (right).

The velocity magnitude contour on the XY plane obtained with Fluent and CFxD is shown in Figure 43.

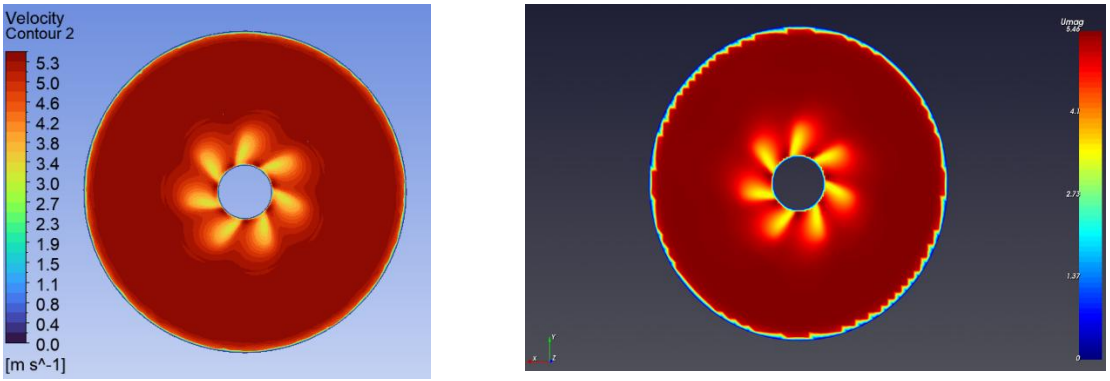

Figure 43. Velocity magnitude contour on the XY plane obtained with Fluent (left) and CFxD (right).

The comparison of the U-velocity profile at 50 mm downstream of the fan is shown in Figure 44.

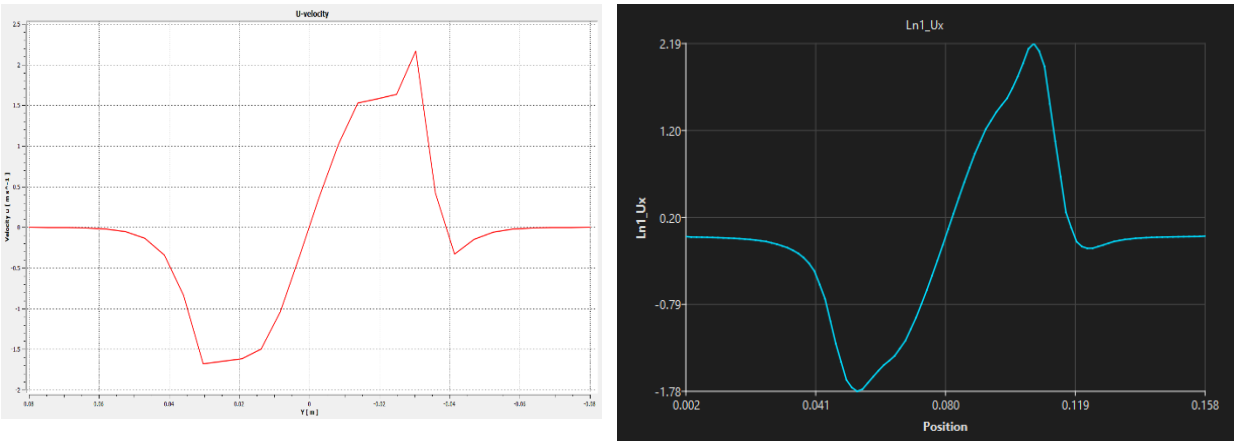

Figure 44. U-velocity profile at 50 mm downstream of the fan obtained with Fluent (left) and CFxD (right).

The comparison of the V-velocity profile at 50 mm downstream of the fan is shown in Figure 45.

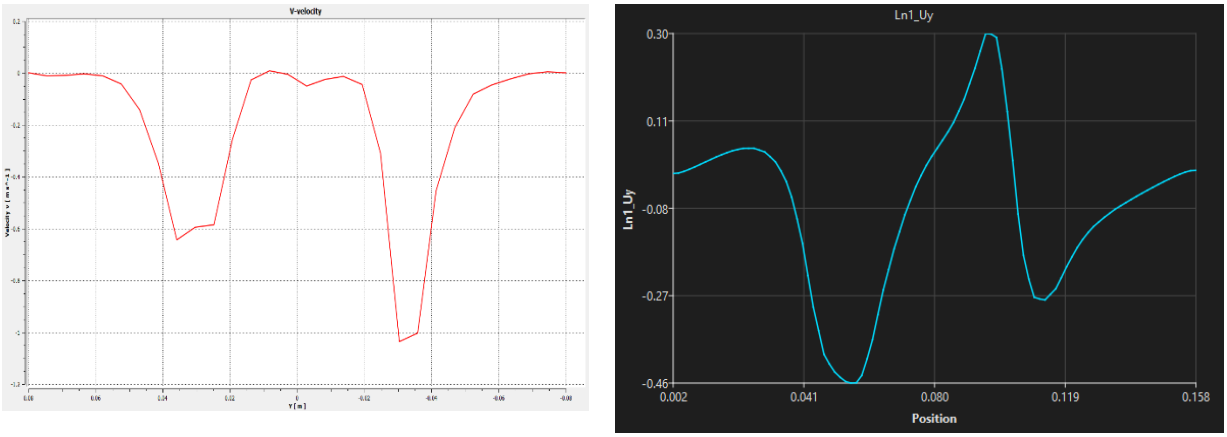

Figure 45. V-velocity profile at 50 mm downstream of the fan obtained with Fluent (left) and CFxD (right).

The comparison of the W-velocity profile at 50 mm downstream of fan is shown in Figure 46.

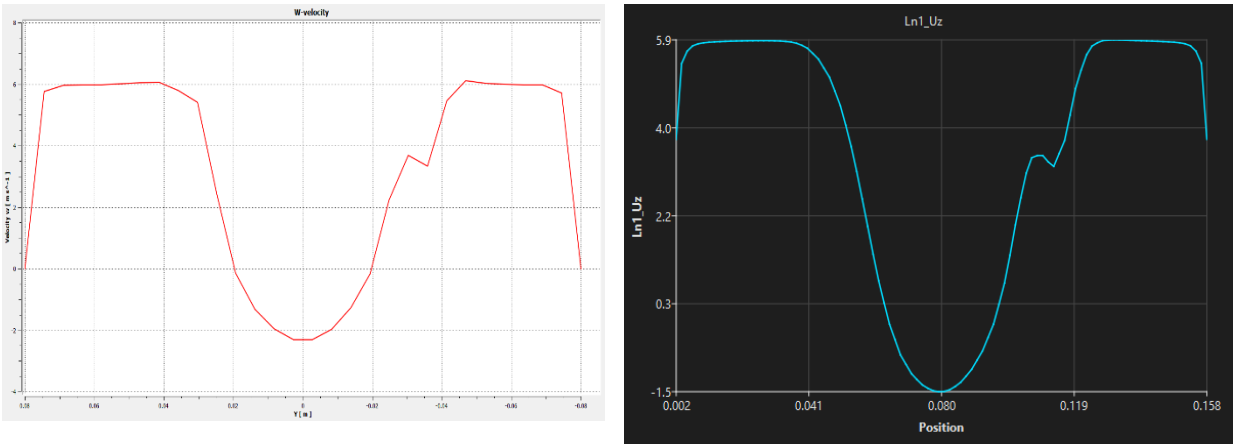

Figure 46. W-velocity profile at 50 mm downstream of the fan obtained with Fluent (left) and CFxD (right).

The pressure force acting on the fan predicted by Fluent is 0.043 N, while the value predicted by CFxD is 0.039 N. The relative difference is approximately 9.3%.

Conclusion

The comparison demonstrates reasonable agreement between the CFxD and Fluent results for airflow through the rotating fan system. Both simulations predict acceleration of the flow through the fan, development of tangential velocity components, and a disturbed wake downstream of the rotating region. The velocity contours show that the principal rotating-flow structures are captured consistently by both software packages.

The U-, V-, and W-velocity profiles at 50 mm downstream of the fan show similar overall trends between the Fluent and CFxD results. The pressure force acting on the fan is predicted as 0.043 N by Fluent and 0.039 N by CFxD, corresponding to a relative difference of approximately 9.3%. The remaining difference may be influenced by mesh resolution around the blades, definition of the rotating-zone interface, pressure integration over the fan surfaces, and numerical treatment of the MRF source terms.

Overall, the results indicate that CFxD provides a consistent prediction for this steady rotating-flow case under the tested mesh, turbulence-model, and MRF settings.

11. Conjugate heat transfer (CHT)

This case models conjugate heat transfer between airflow inside a cylindrical pipe and heat conduction through the pipe wall. The pipe has an inner diameter of 1.0 m and a wall thickness of 0.1 m. The pipe length is 5 m. The inlet velocity is (U = 2) m/s, and the inlet air temperature is 288 K. Air is used as the working fluid, and steel is used as the solid wall material.

The outer surface of the pipe wall is maintained at a temperature of 350 K. Heat is transferred by conduction through the steel wall and by convection from the inner wall surface to the airflow. Temperature and heat-flux continuity are imposed at the fluid–solid interface.

The mesh size used in CFxD is approximately 108 thousand cells, while the mesh size used in Fluent is approximately 106 thousand cells. The SST turbulence model is used for the fluid region in both simulations.

Results and comparison

The velocity magnitude contour on the symmetry plane obtained with Fluent and CFxD is shown in Figure 47.

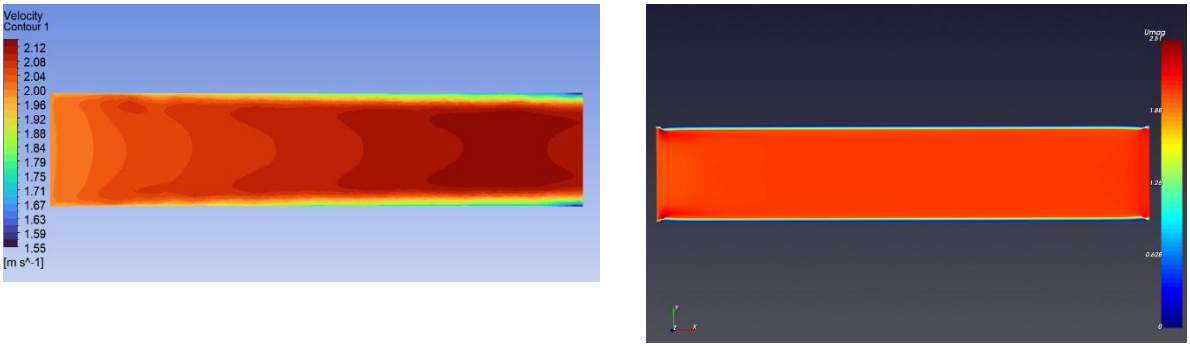

Figure 47. Velocity magnitude contour on the symmetry plane obtained with Fluent (left) and CFxD (right).

The temperature contour on the symmetry plane obtained with Fluent and CFxD is shown in Figure 48.

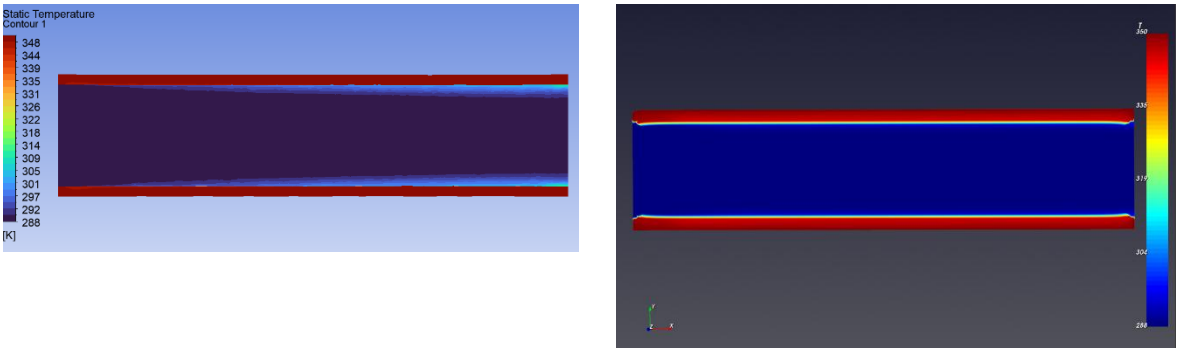

Figure 48. Temperature contour on the symmetry plane obtained with Fluent (left) and CFxD (right).

The comparison of the temperature profile at 4.5 m downstream of the inlet is shown in Figure 49.

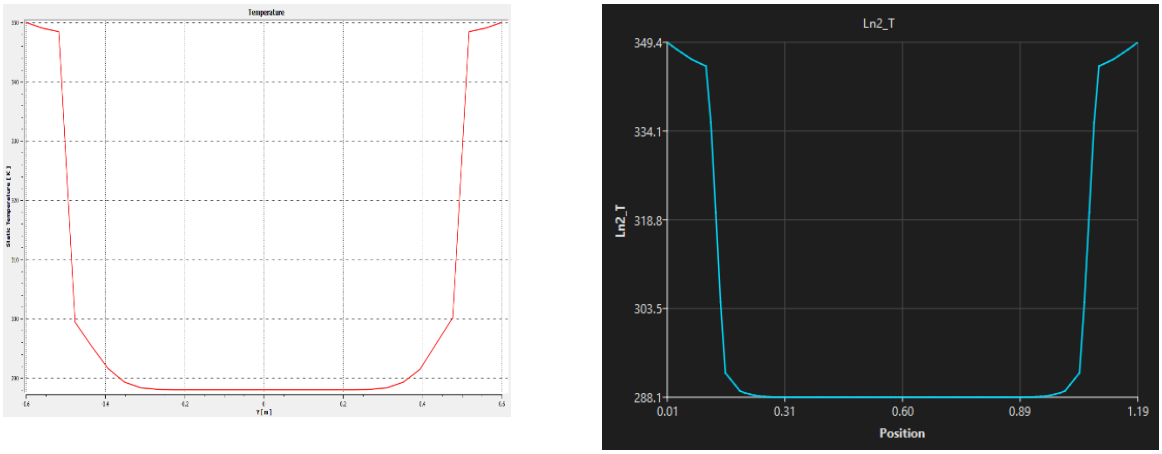

Figure 49. Temperature profile at 4.5 m downstream of the inlet obtained with Fluent (left) and CFxD (right).

Conclusion

The comparison demonstrates good agreement between the CFxD and Fluent results for conjugate heat transfer between the airflow and the steel pipe wall. Both simulations predict heat conduction through the solid wall and convective heat transfer from the inner wall surface to the fluid. The temperature contours show that the main thermal gradients in the solid and fluid regions are captured consistently by both software packages.

The temperature profile at 4.5 m downstream of the inlet shows a similar overall trend between the Fluent and CFxD results. Any remaining differences may result from variations in fluid–solid interface treatment, mesh resolution across the wall thickness, thermal boundary-layer resolution, and thermophysical-property implementation.

Overall, the results indicate that CFxD provides a consistent prediction for this conjugate heat-transfer case under the tested mesh and solver settings.

References

1. Software user guide. (Theory and general overview)
2. Yun A. Computational Fluid Dynamics: from zero to guru. Creative Space, 2019.